Loss of PIF7 attenuates shade and elevated temperature responses throughout the lifecycle in pennycress

Vanessica Jawahir[1], Salma Adam[1], Marcus Griffiths[1], Tad Wesley[2], Win Phippen[2], Nicholas Heller[3], Bhabesh Borphukan[4], Karen Sanguinet[4], and Dmitri A. Nusinow[1†]

[1] Donald Danforth Plant Science Center, Saint Louis, MO 63132, USA

[2] School of Agriculture, Western Illinois University, 1 University Circle, Macomb, IL 61455, USA

[3] Department of Agriculture, Illinois State University, Normal, IL, USA

[4] Department of Crop and Soil Sciences, Washington State University, Pullman, WA 99164, USA

[†]To whom correspondence should be addressed: meter@danforthcenter.org

Abstract

Pennycress (*Thlaspi arvense*) is being developed as a winter annual intermediate oilseed bioenergy crop in the Midwest during typical fallow periods. Crucial work remains to domesticate and optimize pennycress for incorporation into cropping systems and increasing resilience to rising temperatures. We found that increased planting density reduces biomass and hastens time to flowering and maturity, which are associated with shade avoidance responses. In controlled conditions, we found that pennycress elongates in response to foliar shade and increased ambient temperatures (28 ˚C). We applied the knowledge base from *Arabidopsis thaliana* to manipulate genes in the PHYB signaling pathway to simultaneously decrease the shade avoidance response during interseeding and tissue responses to elevated temperatures. Evaluation of CRISPR alleles of PIF7 shows that *pif7* reduces organ elongation to competition and heat cues and retains a compact rosette when exposed to shade or elevated temperature and their combination. Crucially, yield and oil content were unaltered in *pif7* and plants maintained earlier flowering in stress conditions. Furthermore, indicators of plant health, such as hue, chlorophyll indices, and root system architecture, were improved between wild type and *pif7*. This is evidence that plant architecture and physiological health can be uncoupled under competition and heat conditions, supporting our efforts to attenuate morphological responses to environmental cues. We propose this strategy for reducing SAR, improving pennycress performance at high densities, for during interseeding establishment in standing crops, and in a warming climate.

Introduction

Agriculture is tasked with increasing production without expanding land use to sustainably produce feed, fiber, and biofuel for the rapidly growing human population (Ranganathan et al. 2018). The required increases in yield can be achieved by improving crop genetics, increasing planting density, and planting more frequently. Recently, improved yield has come from selecting for tolerance to increased planting densities (Duvick 2005). However, planting densities must be carefully optimized as excessive density plantings trigger the shade avoidance response (SAR), a syndrome resulting from perceived competition for light. SAR, a major limitation to crop planting density, leads to elongated growth, altered tillering, increased lodging, and early flowering, and can result in the underperformance of the shorter species during intercropping (Lu et al. 2023; Li et al. 2021; Tang & Liesche 2017; Liu et al. 2021). Elongation and early flowering are evolutionarily advantageous to increase the fitness of individuals but are undesirable in crop monoculture systems as elongated plants are more prone to lodging, and allocation of resources to these competitive traits often reduces yield (Tang & Liesche 2017; Wille et al. 2017; Raza et al. 2020; Roig-Villanova & Martínez-García 2016; Schmitt et al. 1999).

The effects of SAR have been partially reduced in cereals by breeding for upright leaf angle high in the canopy to better capture light and reduce canopy shading (Wille et al. 2017; Cao et al. 2022). This altered plant architecture allows for significantly increased *Zea maize* planting density from 30,000 plants/hectare to 80,000 plants/hectare, a major factor in yield gains (Duvick 2005; Assefa et al. 2018). Improvements in leaf angle have slowed, suggesting this trait is at near peak optimization in maize (Elli et al. 2023), and increased tolerance to higher planting density will need to be accomplished through alternative mechanisms. Leaf angle is not a uniform target for trait improvement in all crops, especially rosette-forming crops. An alternative strategy is to attenuate SAR and diminish changes that occur in response to high planting density. Studies in *Arabidopsis thaliana* have shown that reduction of SAR improved monoculture performance at high densities and increased weed suppression (Pantazopoulou et al. 2021), supporting that SAR attenuation is a viable strategy.

The molecular mechanism of SAR has been well studied in Arabidopsis and is a rich resource to mine for candidates for targeted improvement. From the Arabidopsis literature, it is understood that plants continually monitor the environment for changes in light quality, quantity,

72 and temperature through phytochromes to initiate transcriptional responses to respond to the
73 environmental signals (Oravec & Greenham 2022; Jung et al. 2016). Signaling through the five
74 phytochromes (phyA to E) in Arabidopsis regulates germination, chlorophyll biosynthesis,
75 photosynthesis, circadian rhythms, shade avoidance, hypocotyl elongation, and flowering times
76 (Sharrock & Quail 1989; Clack et al. 1994; Sharrock 2008; Kami et al. 2010). Phytochromes are
77 converted to the Pfr (active) form upon red (R) (660 nm) light exposure and reverted to the Pr
78 (inactive) form either upon far-red (Fr) (730 nm) light exposure, exposure to elevated
79 temperatures (thermal reversion), or by incubation in the dark in a process termed dark reversion
80 (Rockwell et al. 2006). Active levels of PHYB respond to the R:Fr ratio. R:Fr in sunlight is
81 approximately 1.15 but is reduced in shade as green canopies are effective at absorbing R light
82 but allow Fr to pass through (Franklin & Whitelam 2005; Smith 1982). Thus, a low R:Fr is the
83 cue to an individual that it is being shaded by other plants and should initiate SAR to overtop
84 neighboring plants.

85 Phytochromes also function as thermosensors due to temperature-dependent PHYB
86 thermal reversion from Pfr to Pr, clarifying their role in plant responses to elevated temperatures
87 (Legris et al. 2016; Jung et al. 2016). Arabidopsis grown in warm temperatures (28˚C) display
88 elongated hypocotyls, petioles, and roots, altered leaf angle, and flowers earlier compared to
89 growth at lower temperatures (Delker et al. 2022; Casal & Balasubramanian 2019; Fernández et
90 al. 2016). Thermomorphogenesis and SAR are phenotypically similar in Arabidopsis, due to
91 PHYB's shared perception of light quality and temperature and initiation of a common signaling
92 cascade to regulate growth. Combining warm temperatures and shade has been reported to have
93 synergistic effects on Arabidopsis hypocotyl elongation (Burko et al. 2022).

94 PHYB modulates plant growth through its interaction with PHYTOCHROME
95 INTERACTING FACTORS (PIF) transcription factors to regulate their post-translational
96 sequestration and turnover (Nozue et al. 2007; Jung et al. 2016; Bauer et al. 2004; Lorrain et al.
97 2008; Park et al. 2012; Park et al. 2018; Kim et al. 2024). PhyB in the active Pfr state binds and
98 sequesters PIFs, preventing their ability to induce gene expression. Repression of PIF activity is
99 relieved when the phytochromes are converted to Pr by either far-red light, darkness, or high
100 temperatures, thereby stabilizing the PIFs and inducing elongation programs. The PIFs induce
101 the expression of auxin biosynthesis genes, leading to organ elongation, which alters plant
102 morphology in response to changing light and temperature conditions (Legris et al. 2019; Pham

et al. 2018; Balcerowicz 2020; Li et al. 2012; Sessa et al. 2018). Individual PIFs have both distinct and redundant functions to modulate responses in specific environments, allowing for fine-tuned growth responses (Pham et al. 2018; Balcerowicz 2020). PIF7 participates in the signaling cascade to reprogram developmental responses to both shade and elevated temperatures. In Arabidopsis, *pif7* mutants have reduced hypocotyl elongation in shade, elevated temperatures, and in combination (Burko et al. 2022). Similarly, *Cardamine hirsuta,* a shade and heat-tolerant plant, does not elongate its hypocotyl when grown in shade and elevated temperatures. *C. histura*'s blunted elongation response is attributed to reduced PIF7 availability compared to the shade and temperature-sensitive Arabidopsis (Paulišić et al. 2021), supporting that modulation of PIF7 activity can confer tolerance to shade and elevated temperature. *pif7* mutants also reduce shade-induced leaf hyponasty, resulting in quicker canopy closure, and were superior to wild type at suppressing the growth of invading plants when grown in field-like conditions (Pantazopoulou et al. 2021).

We sought to test if we can simultaneously reduce SAR and thermomorphogenesis by mutating PIF7 in pennycress (*Thlaspi arvense* L.; field pennycress). The pennycress genome is small, diploid, and more than 70% of the predicted peptides of the pennycress genome have more than 80% sequence similarity to those of Arabidopsis (Dorn et al. 2015). Pennycress is in the early stages of domestication as an intermediate oilseed crop with the dual benefit of soil protection during the winter. The September through October planting window is a crucial predictor of yield. Therefore, in northern US regions, growers will likely need to interseed pennycress into standing crops or in crop residue, forcing pennycress seedlings to establish themselves under shaded conditions. Pennycress had superior stand establishment when interseeded into soy rather than maize, which was attributed to higher light quality and light penetration through the soy canopy (Mohammed et al. 2020). We hypothesize that reduced SAR in pennycress will allow for improved intercropping, tolerance to higher planting densities, and greater ground cover during the winter. Altering the pathways regulating SAR could also impact thermotolerance, given they share components, and altered lines could be more tolerant to the fluctuating temperatures in fall and spring. Pennycress is a prime species to test the benefits of reducing SAR since overcoming interseeding challenges is relevant to the crop's success.

In this study, we found that high planting densities negatively impact pennycress biomass and that pennycress responds to shade and elevated temperature. We mutated PIF7 and showed

134 that *pif7* has reduced organ elongation when exposed to shade or elevated temperature, and their
135 combination. At high densities, *pif7* has reduced elongation, supporting that reducing SAR is a
136 promising strategy for improving plant performance at high densities.
137
138
139 **Results**
140 **Planting density affects whole plant morphology and flowering time, but not yield.**
141 Optimizing planting density for any crop is necessary to balance maximal yield potential
142 with competition for nutrients and light. To explore effects of planting density on pennycress
143 morphology and ground cover, ARV1*tt8*, an early commercial pennycress line, was sown in four
144 replicate plots at 3, 5, 7, and 9 lbs per acre in Macomb, IL, in 2023. Morphology traits were
145 monitored throughout the 2023-2024 field season. At maturity, five plants from the center of
146 each plot were harvested to characterize morphological differences. Plants at 3 lbs/acre produced
147 the most tillers and had the highest biomass (Figure 1). Plants sown at 5 lbs/acre or higher
148 developed significantly fewer tillers and had lower biomass. Changes in morphology were also
149 apparent at the rosette stage before plants had entered winter dormancy. Sixty-four days after
150 planting, five rosettes from each plot were harvested and imaged to measure rosette traits and
151 leaf number. Rosettes from each planting density had statistically the same leaf area, but became
152 more elongated at 7 and 9 lbs/acre, reducing solidity (Supplementary Figure 1). A reduction in
153 solidity indicates that there is more space between the leaves as the convex hull contains a lower
154 percentage of plant material.
155 Changes in individual plant biomass were significant in both above- and below-ground
156 biomass. Root cores were collected from the center of each plot 179 days post-sowing, and the
157 number of plants per root core was determined by counting the number of tap roots present in
158 each core. Plots of 5, 7, and 9 lbs/acre had the greatest number of plants per root core, indicating
159 that higher-density plots had more plants. (Supplementary Figure 1). At 3 lbs/a, individual plants
160 had longer total root length, larger average root diameter, and more biomass than plants at higher
161 densities (Figure 1 and Supplementary Figure 1). Overall, we observed reduced root and shoot
162 biomass per plant when grown at higher densities, demonstrating morphological changes
163 secondary to increased planting densities.

164 Pennycress is a dual-purpose intermediate crop with large rosettes that can protect the
165 soil, similar to cover crops. We assessed this secondary benefit of pennycress by determining the
166 percent plant coverage of the total plot area. Drone images of the plots were collected every
167 week starting in February after planting. Percent green coverage was determined by applying a
168 color threshold to calculate the plot percentage covered by plant versus bare soil. The first drone
169 images at day 149 post-sowing are representative of the percent plot protection during the
170 majority of the winter months, with minimal above-ground growth during this time. There were
171 no statistical differences in percent green coverage for all planting densities on day 149, and all
172 time points after day 187 post-sowing (Supplementary Figure 1). The higher planting densities
173 had greater overall percent green cover during the growth and bolting phase. Green cover
174 plateaued after 200 days post-sowing and began to decrease starting day 235 post-planting, likely
175 due to senescence at maturity.
176 Plots at all densities began to open flowers at day 180 post-sowing. Plots sown at 7 and 9
177 lbs/acre reached 50% and 100% flowering earlier than the 3 lbs/a plots. At maturity, all plots
178 were harvested, and the average yield from all plot densities was statistically the same. This
179 indicates that increasing pennycress planting density above 3 lbs/a does not increase yield per
180 plot (Figure 1). We hypothesize that the morphological responses seen at higher densities reduce
181 per-plant yield and indicate plant competition within the plot.
182
183 **Pennycress elongates in response to shade and elevated temperatures.**
184 The reduced tillering and early flowering phenotypes seen at high densities (Figure 1) are
185 indicative of SAR and occur in the presence of canopy and neighbor shade in shade-intolerant
186 plants (Wille et al. 2017; Franklin 2008; Cerdán & Chory 2003). Therefore, we hypothesized that
187 pennycress is shade intolerant. Pennycress responses to shade were measured in the MN106
188 reference background as this line has a sequenced genome (Dorn et al. 2015; Nunn et al. 2022).
189 Hypocotyl elongation was measured for seedlings germinated in white light, then supplemented
190 with far-red light to reduce the Red:Far red (R:FR) from 2.1 to 0.2 during the day. Seedlings
191 increased hypocotyl length under shade (Figure 2).
192 The photomorphogenic response to shade led us to hypothesize that the red-light
193 signaling pathway likely underlies the SAR phenotypes in pennycress and may be initiated by
194 PHYB. Since PHYB co-senses temperature in Arabidopsis, we investigated how pennycress

195 responds to a moderately elevated temperature (28 °C) and the interaction of shade and
196 temperature ((Burko et al. 2022; Romero-Montepaone et al. 2020; Casal & Fankhauser 2023).
197 Pennycress increased hypocotyl length at 28 °C, and when in combination with shade (Figure 2).
198 Hypocotyls elongated the most in heat alone, while the combination of shade and heat resulted in
199 an intermediate length between the average length seen in the individual treatments of shade and
200 heat. The response to combined heat and shade contrasts with the additive effect observed in
201 Arabidopsis (Burko et al. 2022), suggesting that pennycress responses to light and temperature
202 are distinct.
203 Pennycress rosettes were exposed to the various environmental conditions to determine
204 how shade and heat impact other developmental stages. Wild-type pennycress was germinated
205 and grown under control conditions for seven days, then maintained under white light or grown
206 under shade, heat, or shade and heat, for an additional seven days. Shade, heat, and shade and
207 heat-treated plants had increased rosette perimeter (Figure 2) and convex hull area, but lower
208 solidity compared to control conditions (Figure 4), indicating that rosette morphology changes in
209 response to the environment. The changes in rosette morphology are attributed to the increased
210 petiole length of leaves when grown under treatment conditions.
211 Light quality and temperature are critical environmental cues that influence flowering,
212 and SAR or higher heat can lead to earlier flowering as a competitive or escape response
213 (Wollenberg et al. 2008). Effects of shade and temperature on pennycress flowering time were
214 determined by germinating seeds for one week under white light, vernalizing for three weeks,
215 then moving to white light for four days before starting shade and/or heat treatment for fourteen
216 days. Shade and heat-treated plants bolted earlier than plants grown under control conditions,
217 demonstrating that pennycress alters flowering time in response to environmental cues (Figure
218 2).
219 We conclude that pennycress exhibits SAR phenotypes of organ elongation and early
220 flowering, indicating that pennycress is a shade-avoidant species. Together, these experiments
221 support that pennycress alters morphology in response to elevated temperatures and foliar shade,
222 and the aberrant morphology seen at high planting densities may be due, in part, to SAR. Next,
223 we targeted SAR and thermomorphogenesis pathways to determine if we could alter pennycress
224 responses.
225

226 ***pif7* has attenuated responses to foliar shade and heat throughout its lifespan.**

227 To test if mutating PIF7 could manipulate SAR and thermomorphogenic pathways in
228 pennycress, we sought to use gene editing to disrupt *PIF7* in pennycress. Genomic analysis
229 identified a likely *T. arvense PIF7* homolog (TaPIF7). TaPIF7 has 80% nucleotide similarity and
230 over 90% amino acid conservation compared to *Arabidopsis thaliana* PIF7 (AtPIF7)
231 (Supplemental Figure 3). We generated PIF7 mutants in MN106 with CRISPR-Cas9 targeting
232 the second exon and the bHLH domain (Figure 3). Sequencing the *PIF7* locus identified mutant
233 alleles in transgene-free homozygous mutant lines. *pif7-1* is a deletion of 242 bases that removes
234 75 amino acids and disrupts the bHLH domain. *pif7-2* is a deletion of 86 bases, which results in a
235 protein that is 122 amino acids instead of 364 amino acids. Due to the severe mutations of *pif7-1*
236 and *pif7-2*, we hypothesize that these are knockout alleles. Importantly, both *pif7* alleles similarly
237 reduced hypocotyl elongation in shade, heat, and shade and heat combined, compared to wild
238 type (Figure 3).

239 To investigate how loss of PIF7 impacts diverse germplasm, we mutated PIF7 in other
240 pennycress genetic backgrounds. Spring32, a wild-type spring ecotype line, and ARV1*tt8*, an
241 early-generation winter ecotype commercial line, were transformed with the CRISPR-Cas9
242 constructs targeting PIF7. Strikingly, the *pif7-1* allele was regenerated in both Spring32 and
243 ARV1*tt8*, as well as additional alleles of *pif7* (Figure 3B and Supplemental 3). $pif7\text{-}1_{S32}$ and
244 $pif7\text{-}1_{ARV1}$ mutants reduced hypocotyl elongation in heat in comparison to their parental lines
245 (Figure 3 and Supplemental 3), supporting that the *pif7* phenotype is not unique to the MN106
246 background and could be useful when introduced into elite breeding lines.

247 We further characterized the *pif7-1* in the MN106 background to determine if *pif7* had
248 attenuated SAR and thermomorphogenesis across developmental stages, tissues, and flowering
249 time. Rosette morphology was compared between wild type and *pif7-1* in shade, elevated
250 temperature, and combined conditions for 14 days. *pif7-1* was similar to wild-type under control
251 conditions, remaining compact with high solidity, reflecting that *pif7* does not stunt growth in
252 control conditions (Figure 4). When exposed to shade, heat, and the combined conditions, wild-
253 type plants increased rosette convex hull area and reduced solidity (Figure 4). In comparison,
254 *pif7* had reduced convex hull area and increased solidity when compared to wild type under
255 shade, heat, or the combined treatments (Figure 4). Comparison of petiole length of dissected
256 rosettes found that *pif7-1* petioles were shorter compared to wild type under all conditions

257 (Figure 4 and Supplemental Figure 4). The elongation was most prominent in the oldest true
258 leaves as they have been exposed to environmental stress for the longest time. The reduced
259 petiole length of each *pif7* leaf results in an overall more compact plant in shade and elevated
260 temperatures.

261 We sought to holistically characterize the impact of mutating *pif7* on plant growth and
262 responses to the environment. Shade and temperature also affect root development, as plants
263 allocate more resources to above-ground growth under these conditions (Salisbury et al. 2007;
264 Rosado et al. 2022; van Gelderen et al. 2018; Gray & Brady 2016). Analysis of the root system
265 found that total root length remained comparable for wild-type plants grown in all conditions,
266 while *pif7-1* had increased total root length in shade, heat, and combined conditions (Figure 4).

267 Chlorophyll fluorescence indices are associated with physiological health and stress
268 levels (Arief et al. 2023; Ghosh et al. 2023; Murchie & Lawson 2013; Stamford et al. 2023) and
269 were used to estimate the impact of shade, heat, and combined conditions on wild-type and *pif7-*
270 *1* health. We measured normalized difference vegetation index (NDVI), chlorophyll index-red
271 edge (CIRE), maximum efficiency of photosystem II (F_v/F_m), and non-photochemical quenching
272 (NPQ), in wild type and *pif7* grown under shade and heat conditions. Wild type reduced NDVI
273 and CIRE in shade and heat conditions, conveying that these environments may lower
274 chlorophyll content (Figure 4). Both NDVI and CIRE measurements were higher in *pif7-1* than
275 wild type in the same environmental condition, suggesting that *pif7-1* is less sensitive to
276 environmental influences on chlorophyll content (Figure 4). By contrast, the average F_v/F_m of
277 wild type and *pif7-1* in all conditions is within the typical range expected of healthy plants
278 (Supplemental Figure 5) (Murchie & Lawson 2013). Similarly, NPQ increased in shade and heat
279 conditions for wild type and *pif7* mutants, suggesting that plants are activating protective
280 mechanisms to prevent damage from ROS, but is comparable between genotypes (Supplemental
281 Figure 5).

282 To determine the effects of *pif7* on pennycress morphology, flowering time, and
283 inflorescence architecture, wild type and *pif7-1* were compared under fourteen days of treatment.
284 *pif7-1* bolted earlier under shade, heat, and in combined conditions compared to the control.
285 However, *pif7* was delayed in flowering by 1-2 days compared to wild type in all conditions
286 (Figure 5). At maturity, height was measured to determine if *pif7-1* affected overall plant height.
287 Wild-type plants were taller in shade, heat, and combined conditions than when in control

288 conditions. Mature *pif7-1* plants grown in experimental conditions were also taller than in control
289 conditions, but remained over 10% shorter than wild-type in the comparative condition (Figure
290 5). This indicates that two weeks of shade and warm temperatures have a lasting impact on plant
291 architecture, and that *pif7* attenuates their physiological impacts.
292
293 ***pif7* does not reduce seed oil content, yield, or freezing tolerance.**
294 Pennycress is grown for its seed oil content, so we compared seed traits of *pif7-1* to wild-
295 type plants grown in all conditions. *pif7-1* did not alter total yield or thousand seed weight
296 (TGW) of plants when transiently treated for 14 d during vegetative growth (Supplementary
297 Figure 6). Seed oil content on a dry weight basis (DWB) was also unaltered in *pif7-1*. This
298 indicates that mutations in PIF7 do not negatively affect yield or oil content (Supplemental
299 Figure 6).
300 In Arabidopsis, PIF7 is known to have additional roles in abiotic stress and is a known
301 negative-regulator of DRE-Binding1, a transcription factor important for low-temperature
302 responses (Kidokoro et al. 2009; Lee & Thomashow 2012). PIF7 repression of DREB1 is
303 hypothesized to reduce expression of cold tolerance genes in unstressed conditions and prevent
304 DREB-induced growth reduction. We tested cold and freezing tolerance, as it is crucial for
305 pennycress winter survival as an intermediate crop. *pif7-1* survived freezing challenges similarly
306 to wild type (Supplementary Figure 7), suggesting that loss of PIF7 did not affect cold tolerance
307 up to –10 ˚C.
308
309 ***pif7* has reduced elongation in low light**
310 If intercropped, pennycress will experience low light and shaded conditions as ground
311 level light intensity (fluence rate) and quality (R:Fr) are both reduced in standing corn and dried
312 soybeans (Supplemental Figure 2). In standing corn, light intensity was decreased nearly 10-fold
313 from approximately 1000 µmol m^{-2} s^{-1} down to 100 µmol m^{-2} s^{-1}. In standing green corn, the R:Fr
314 was also lowered from 1.4 to 0.6 at ground level. Light conditions in standing corn are various
315 and complex, and are a significant hurdle to overcome during intercropping. We sought to
316 explore any effects of low light intensity on pennycress in a controlled environment.
317 Elongation of wild type and *pif7* was measured in both seedlings and rosettes when
318 exposed to low light. Hypocotyl elongation in response to a titration of light intensity found that

both *pif7* mutants elongated hypocotyls less than wild type in response to reduced light intensity at 20 µmol m^{-2} s^{-1} to 45 µmol m^{-2} s^{-1} (Figure 5). Elongation in low light was also assessed at the rosette stage. Wild type and *pif7-1* were grown under the recommended control light intensity, 300 µmol m^{-2} s^{-1}, and low light, 80 µmol m^{-2} s^{-1}. Similar to the results for hypocotyl elongation, *pif7-1* elongates petioles less than wild type when grown in low light.

pif7 has reduced elongation at high density without impacting yield

To assess if reducing SAR enhances pennycress performance at high densities, *pif7-1* was sown in mini-fields at seeding rates of 5 and 10 lbs per acre and monitored through senescence. The mini-fields were vernalized at 4 °C for 3 weeks following a two-week germination and establishment period. After vernalization, the mini-fields were returned to the greenhouse and imaged every five days to monitor ground cover and flowering time. As expected, mini-fields sown at 10 lbs/a had a higher ground cover percentage than 5 lbs/a. All genotypes and planting densities reached around 90% green coverage at 15 d post-vernalization (Figure 7).

Density and genotypic effects on individual plant morphology were assessed at 11 days post-vernalization. This time point was chosen to capture rosette morphology when mini-fields had high green cover, ensuring neighboring plants were touching, but before plants transitioned to flowering. Wild-type rosettes at 10 lbs/a had increased convex hull area and perimeter, but reduced solidity compared to 5 lbs/a (Figure 7). In contrast, *pif7-1* rosettes maintained their rosette shape at both planting densities, as convex hull area, solidity, and perimeter are not statistically different between 5 lbs/a and 10 lbs/a (Figure 7).

All mini-fields had open flowers at 30 d post-vernalization, with wild type at 10 lbs/a averaging the most inflorescences with open flowers. All mini fields reached 100% flowering at 40 days post-vernalization, but varied in the number of inflorescences (Figure 7). *pif7* mini-fields appeared healthier than wild type at both planting densities and flowered uniformly. The center of each wild-type mini-field yellowed and failed to flower at both planting densities; plants along the perimeter were the only ones that flowered, while *pif7-1* had overall less yellowing and clearings. Yield remained statistically the same for wild type and *pif7-1* at all planting densities, showing that reducing SAR responses does not decrease yield.

350 **Discussion**

351 Here we show that mutating PIF7 reduced SAR and thermomorphogenesis in pennycress
352 with limited impacts on plant health, yield, and seed oil content. Reducing SAR through gene-
353 editing is a rapid and promising strategy to increase crop performance at high-density plantings
354 in diverse environments. *pif7* grown in high-density monocultures elongated less and had more
355 flowers than wild type, demonstrating reduced plasticity to the surrounding environment. This
356 reduced plasticity will increase uniformity of plant growth across millions of acres, even while
357 facing various environmental challenges within different hardiness zones. Increasing planting
358 density has been one of the most effective strategies to increase yield. As leaf angle
359 optimizations have slowed (Elli et al. 2023), planting density improvements will need to be
360 accomplished through alternative mechanisms. Superior vegetative architecture varies greatly
361 between species, and will require unique identification and optimization of genetic influences of
362 each specific trait. Alternatively, reducing the capability of plants to change their architecture in
363 response to high-density plantings is a more broadly applicable strategy. Coupling superior
364 architecture with reduced responses to neighbor competition could be paramount to maximize
365 plant performance at high densities. This study demonstrates the viability of attenuating SAR to
366 control plant architecture and physiological traits.

367 Pennycress is currently in the early stages of domestication and presents an opportunity
368 to create a variety suited for use across the US agriculture zones. Widespread adoption of
369 pennycress could produce enough material to convert to fuel to meet the 35 billion gallons of
370 sustainable aviation fuel mandate. Pennycress oil has a fatty acid composition well-suited for
371 conversion to biodiesel and biojet fuel, meets the U.S. Renewable Fuels Standard (Fan et al.
372 2013), and can produce 600 liters ha^{-1} (65 gal ac^{-1}) of oil annually without competing for land
373 use with food crops (Moser et al. 2016; Moser 2012). This, combined with ecosystem services
374 provided by growth over the winter when fields typically lay fallow, positions pennycress as a
375 strong candidate crop to meet our future mandated sustainable aviation fuel goals (Fan et al.
376 2013; Griffiths et al. 2022).

377

378 **Pennycress responds to high-density plantings and environmental cues**

379 Here, we have shown that both above- and below-ground biomass was negatively
380 impacted by high-density plantings in the early commercial line ARV1*tt8* and did not increase

381 yield (Figure 1 and Supplemental Figure 1). Further analysis in controlled conditions showed
382 that pennycress is shade and heat-intolerant and responds to simulated canopy shade by
383 elongating organs and flowering earlier. Elongated petioles at the rosette stages increase rosette
384 perimeter and convex hull area, and expose more soil between the leaves (Figures 2, 4). Etiolated
385 plants reduce robust stand establishment and will decrease soil coverage in the field, thereby
386 lowering the potential ecosystem benefits of weed suppression and soil preservation by planting
387 pennycress (Griffiths et al. 2022; Pantazopoulou et al. 2021). The elongation phenotypes in our
388 controlled environments were similar to those in high-density field plots, suggesting that
389 pennycress SAR underlies some physiological alterations seen with increasing density.
390 Light quality and quantity are both reduced at ground level in fields with a standing crop,
391 which may reduce pennycress stand establishment when intercropped (Supplemental Figure 2).
392 Elongation in response to low light and shade may limit the ability to intercrop current
393 pennycress varieties into existing corn and soy rotations, particularly in northern states where
394 summer crops are often not harvested before September. Delaying pennycress planting until after
395 corn harvest can negatively impact yield (Cubins et al. 2019; Dose et al. 2017; Patel et al. 2021;
396 Bishop & Nelson 2019), but earlier planting can be challenging as temperatures continue to
397 increase during the fall in the Midwest (Us Epa 2021), triggering thermomorphogenesis.
398
399 **Altering pennycress morphology by perturbing PHYB signaling**
400 We sought to simultaneously reduce SAR and thermomorphogenesis by manipulating the
401 PHYB signaling pathway and targeted PIF7 as it plays dual roles in elongation to shade and
402 temperature (Burko et al. 2022; Fiorucci et al. 2020; de Wit et al. 2016; Galvão et al. 2019;
403 Paulišić et al. 2021). CRISPR alleles were generated in multiple backgrounds, including a first-
404 generation commercial line. Interestingly, we generated an identical allele, *pif7-1*, in all three
405 backgrounds. This feat demonstrates that gene editing can generate identical alleles, likely
406 through repair of breaks through microhomology (Schiml et al. 2016).
407 The wild-type lines (MN106, Spring32, and ARV1*tt8*) all elongated in heat, but to
408 varying degrees. The variability in elongation response suggests that there is natural phenotypic
409 variability to heat, and yet all PIF7 mutants reduced hypocotyl elongation in response to
410 temperature (Figure 3 and Supplemental Figure 3). This evidence also supports the hypothesis
411 that PIF7 is a viable candidate for manipulation across pennycress genetic backgrounds. Further

412 analysis showed that *pif7* alleles in the MN106 background had comparably reduced hypocotyl
413 elongation to shade, heat, and their combination. In summary, our study implies that PIF7 is part
414 of a shade and elevated temperature signaling cascade affecting plant development.
415 *pif7-1* attenuated petiole elongation, flowering time, and inflorescence stature compared
416 to wild type in all treatment conditions (Figures 4 & 5). Shade and heat alone, or in
417 combination, continued to shorten the flowering time in *pif7-1* compared to wild type in control
418 conditions (Figure 5). The slight impact on flowering is critical to ensure compatibility of this
419 crop with the planting of summer cash crops. Pennycress holistically responds to the
420 environmental cues by altering root growth, similar to Arabidopsis (Rosado et al. 2022; van
421 Gelderen et al. 2018). Diversion of critical resources to shoot growth is hypothesized to enhance
422 competitiveness in suboptimal light quality. Interestingly, *pif7* continues to increase total root
423 length in shade and elevated temperature, suggesting it has dampened the competitive growth
424 reprogramming response to shoots while increasing root length (Figure 4). Greater root length
425 enhances plant resource capture of water and nutrients by increasing soil exploration and root-
426 soil contact, thereby improving plant resilience and nutrient catch as a cover crop (York et al.
427 2013; Griffiths et al. 2022).
428
429 **Pennycress health and yield is not strongly impacted by shade and temperature**
430 Elongation is a strategy to outgrow shade-casting neighbors or to protect organs from hot
431 soil. We found that *pif7* or reduced SAR does not negatively impact yield and plant health. This
432 study sought to understand if elongation provided a physiological benefit to plants in our test
433 environments by measuring chlorophyll indexes commonly used to assess plant stress (Murchie
434 & Lawson 2013; Maxwell & Johnson 2000; Arief et al. 2023). Wild-type and *pif7-1* individual
435 plants had similar F_v/F_m measurements near the idealized 0.8 measurement in control conditions,
436 shade, heat, and shade plus heat, indicating that these conditions are not stressful enough to
437 damage PSII (Supplemental Figure 5). NPQ is a protective mechanism that increases when
438 plants experience high light or other abiotic stresses (Ghosh et al. 2023; Murchie & Lawson
439 2013; Stamford et al. 2023). NPQ increased similarly in the test conditions between wild type
440 and *pif7-1*, suggesting that these plants are activating protective mechanisms to prevent damage
441 from ROS, and this response is preserved in *pif7* (Supplemental Figure 5). Similarly, seed
442 quantity, weight, and oil content were not significantly altered in *pif7* compared to wild type in

443 control and experimental conditions (Supplemental Figure 6). These data support the idea that
444 *pif7* does not reduce yield.
445 Overall, we did not find evidence of growth or photosynthetic impairment in *pif7*, as *pif7-*
446 *1* remained comparable to wild type when grown in control conditions. We believe *pif7* does not
447 have a significant negative effect outside of suppressing SAR and heat responses, and therefore
448 this mutation is viable for integration into elite breeding lines.
449
450 **The potential for *pif7* to improve interseeding.**
451 Low light intensity and shade are critical challenges for pennycress establishment in
452 intercropping scenarios (Supplementary Figure 2). When interseeded into standing corn,
453 pennycress will face the complex environment of low fluence and low R:Fr (Supplementary
454 Figure 2). The etiolated morphology that pennycress adopts when grown in standing corn is
455 hypothesized to contribute to poor establishment and reduced yield (Supplemental Figure 2).
456 Reducing elongation in low light and shade may improve interseeding success. Our study
457 demonstrates that, in controlled low fluence environments, pennycress phenocopies morphology
458 in reduced R:Fr by similarly elongating hypocotyls and petioles (Figure 5). *pif7* had reduced
459 hypocotyl and petiole elongation in low light compared to wild type and was not allele specific.
460 Our data is the first to implicate *pif7* function in low fluence and suggests that canonical red light
461 signaling has a role in growth responses to low fluence. This novel finding implicates the PHYB-
462 PIF signaling hub as a regulator of morphology responses to low light.
463
464 **Potential to increase planting density**
465 Our ultimate goal is to reduce the undesirable morphogenic changes associated with
466 SAR, allowing plants to maintain ideal architecture when grown at high density. We tested *pif7*
467 performance in a common garden experiment by sowing mini-fields at 5 lbs/a and 10 lbs/a, both
468 densities higher than the recommended 3 lbs/a, in a temperature-controlled greenhouse. Our
469 mini-field experiments also showed that *pif7* had reduced rosette elongation at 10 lbs/a and is
470 statistically the same as wild type at 5 lbs/a in rosette morphological characteristics (Figure 7).
471 This shows that SAR and light quality contribute to the elongated phenotypes seen at high-
472 density plantings. The *pif7* mini-fields looked healthier than wild type due to yellowing and
473 flowered uniformly in the mini-fields. Importantly, yield was not decreased by mutating *pif7,*

474 supporting a hypothesis that we can improve vegetative growth responses to the environment
475 without a yield drag.
476
477 **Summary**
478 We have used the foundational knowledge from the Arabidopsis red-light signaling
479 pathway to reduce plasticity to environmental cues in pennycress. Creating a PIF7 mutant
480 resulted in attenuated elongation in shade and elevated temperatures, and under low light
481 intensities associated with interseeding. This study supports that reducing SAR is a promising
482 strategy to optimize plants for planting under challenging conditions found during intereseeding
483 and at higher densities.
484
485 **Methods**
486 **Plant materials**
487 MN106 is the primary wild-type line used throughout the paper, and Spring32 and
488 ARV1*tt8* are additional germplasm used to generate additional PIF7 mutants. ARV1*tt8* is an
489 early commercial line with a mutation in TRANSPARENT TESTA 8 (Koirala et al. 2023). *pif7-*
490 *1* is a novel allele generated in MN106, Spring32, and ARV1*tt8* backgrounds. *pif7-2* was an
491 additional allele generated in the MN106 background, while *pif7-3* was generated in Spring32
492 background and *pif7-4* was generated in the ARV1*tt8* background. All alleles were developed
493 using CRISPR gene editing as described below. MN106 is the parental background unless
494 otherwise denoted with a subscript.
495
496 **Field trials**
497 The field trial was conducted at Western Illinois University in Macomb, IL, USA
498 (40.4885, -90.6902). The preceding crop was Cereal rye, which was harvested on June 26th,
499 2023. 50lb. N (28% UAN)+ 10lbs. Sulfur (Thiosulfate) was applied as a liquid on September
500 26. Treflan was applied on all plots at a rate of 1 qt./acre and double incorporated with tillage.
501 Seed was prepared into planting packets. Pennycress seed was broadcast on September 29th,
502 2023, with ½ inch of water applied within 24 hours of planting. Plots were 4’ x 10’ in size and
503 sowed at 3, 5, 7, and 9 lbs/acre.

Five rosettes were removed from each plot 64 days after planting on December 04, 2023, after plants slowed their growth. Rosettes were imaged with an overhead camera to analyze rosette morphology.

On May 15, 2024, at maturity, five whole plants from the center of each plot, including the root system, were harvested. All plants were individually imaged. The number of tillers arising from the basal rosette was manually counted. Plants from the same plot were dried and weighed as a group to calculate biomass.

One soil core was taken from the middle of each plot and directly over one plant, ensuring that the cored section represented the whole plot. Soil cores were taken from the field on March 27th, 2024, 179 days post-planting using a bulb and garden planter with 6” depth x 3” diameter dimensions. Cores were placed in plastic bags and stored at -20 °C until washing. After defrosting in a water bath, the soil cores were carefully washed by hand, and the roots cleaned and separated from particulate organic matter. Washed roots were then stored in clean plastic bags at 4 °C and were imaged in the following days using an Epson Expression 12000XL flatbed scanner equipped with a transparency unit (Epson America Inc, Los Alamitos, CA, USA). Roots from the soil core were carefully separated in a water-filled plastic tray into individual plants by the tap root. Roots were placed on square plates (150 mm × 150 mm) filled with a 10 mm layer of deionized water with one tap root per tray. Unconnected roots from neighboring plants that had no tap root were placed in a separate square plate. All roots were spread out using forceps to avoid overlap between roots. Six trays were imaged simultaneously with the scanner using the Epson Scan 2 software (Epson America Inc, Los Alamitos, CA, USA) at a resolution of 600 dpi as a JPG file with 99% quality. The individual root images were cropped out of the main image, and root measures were computed using RhizoVision Explorer v2.0.2 (Seethepalli et al. 2021). In the software, the tap root length, lateral root length, and tertiary root length were classified by root diameter threshold ranges of > 0.4 mm, 0.4 - 2 mm, and < 2 mm, respectively. The image thresholding level was set to 200, and the root pruning threshold was set to 20 pixels. After scanning, the root material was placed in a paper envelope and dried at 60 °C. In this way, root length density for the plot was determined after aggregating individual plant data together by core. Root length per plant was determined by averaging the root measures by number of tap roots per plot.

535 **Drone Imaging and Analysis**

536 Drone images were taken after the hard frost period throughout the spring to harvest
537 starting on February 27, 2024, and finishing on May 27, 2024. The whole field was imaged every
538 7 to 10 days with 12 flights. The drone used for data collection was a DJI Mavic 3M equipped
539 with a multispectral sensor camera. Flights were pre-programmed using DJI Pilot 2 and were
540 conducted at 17 m height above the ground with an image resolution of 0.75 cm/pixel. Images
541 were collected at an approximate flight speed of 1.5 m/s. There was 70% side overlap and 80%
542 frontal overlap in the collected images. The time of the day for each flight was around 9 am
543 CDT, ensuring the weather conditions were similar. Images were assembled into orthomosaics
544 using WebODM v. 2.5.

545 Image analysis was conducted on the orthomosaic images using a custom Open-CV
546 Python code (Griffiths 2025). A reference scale was established for each orthomosaic using the
547 known field distance, and a scaling factor was applied to ensure consistent dimensions across
548 plots. Then the images were rotated, ensuring each image had the same orientation. Individual
549 plots were then cropped out as a grid layout, and plot names were assigned to the images. To
550 differentiate between bare soil and vegetation, a soil mask was generated using the Blue-Green
551 Index (BGI). Pixels with BGI < 0.15 were classified as soil. Additionally, a green leaf index
552 (GLI) was used to differentiate green and senesced vegetation based on a GLI threshold of 0.2
553 (>= 0.2 green, < 0.2 senesced). The indices used are defined as:

554 $BGI = (G - B) / (G + B + \varepsilon)$, $GLI = (2 * G - R - B) / (2 * G + R + B + \varepsilon)$

555 Where R, G, and B are the red, green, and blue channels of the image, respectively, and ε is a
556 small constant to avoid division by zero. The percentages of green tissue and senesced tissue
557 were calculated relative to the total pixel count within the plot. To ensure accurate cropping and
558 thresholding, a reference image was generated for each plot by overlaying the indices on the
559 original orthomosaic for manual validation.

560

561 **Seed sterilization and growth conditions**

562 Seeds were sterilized with a 30% bleach and 0.1% Triton solution for 15 minutes and
563 washed three times with sterile water. For bulk sterilization, seeds were gas sterilized by
564 arranging seeds in a single layer and exposed to chlorine gas for 5 hrs. Seeds were plated on ½
565 strength Murashige and Skoog (MS) medium and stratified at 4 °C for 3-5 d. Plates were grown

566 at 130 µmol/m-^{2}/s^{-1} in 12:12 light:dark cycles at 22 °C for 4-7 d then vernalized at 4 °C with
567 12:12 light:dark for 3 weeks, unless otherwise noted.
568 Hypocotyl measurements were taken by growing seeds for 2 d at 22 °C 12:12 light:dark
569 control conditions, then exposed to the experimental conditions for the indicated number of days.
570 White light conditions were a 12 hr day/ night at a constant 22 °C. For heat treatment, plates
571 were grown at 28 °C during the day with a 12 hr day/night cycle and 22 °C night temperature.
572 Canopy shade was simulated by adding a far-red light during the daytime to reduce the R:Fr to
573 0.3. A constant temperature of 22 °C was maintained at plant level by reducing the chamber
574 settings to 20 °C during the day to compensate for the heat given off from the far red lights. For
575 the shade + heat treatment, plates were incubated under far red light during the day at an R:Fr of
576 0.3. A daytime temperature of 28 °C was maintained by adjusting the chamber to 25 °C during
577 the day when the supplemental far red lights were on and the night temperature was 22 °C.
578 Temperature readings were collected with a HOBO meter to ensure chambers were at the proper
579 temperature.
580 Plants grown for rosette measurements were sown directly into soil in 3.5 in pots. Light
581 intensity was 200 µmol/m-^{2}/s^{-1} with a 16:8 light/dark cycle at 22 °C. Plants had to have visible
582 true leaves before beginning experimental conditions. A daytime temperature of 28 °C was the
583 heat treatment. Shade was simulated with the addition of far red to reduce the R:Fr to 0.3. The
584 chamber temperature was set to accommodate the heat generated by the far red lights, which was
585 22 °C (shade only) or 28 °C (shade + heat), and night temperatures were 22 °C. Rosettes were
586 imaged on the indicated day.
587
588 **Plant transformation and selection**
589 Plants were transformed using *Agrobacterium tumefaciens* strain GV3101 by submerging
590 inflorescences in an Agro solution, then vacuum infiltrated under 27 inches of mercury for at
591 least 10 minutes (McGinn et al. 2019). Inflorescences were wrapped with cling wrap and placed
592 in the dark overnight. In the morning, plants were returned to standard growth conditions and
593 allowed to mature.
594 T_1 seeds were selected by growing on 50µg/mL of hygromycin for 2 weeks. Resistant
595 plants were vernalized and rescued to soil. Plants were genotyped to confirm the presence of
596 CRISPR and mutations to the target gene.

597

598 **Generating CRISPR alleles**

599 Two guide RNAs were designed with Cas-designer (Park et al. 2015) to target the PIF7
600 coding region. Guide RNAs (gRNA) were cloned into a pHEE401 CRISPR-containing vector as
601 described. The first gRNA with PAM sequence is TCTTGGGCGTCTTTCGAATCTGG. The
602 second gRNA plus PAM sequence is CGATTCACAACGAGTCTGAAAGG. The pHEE401
603 containing gRNAs and CRISPR was transformed into pennycress lines: MN106, Spring 32, and
604 ARV1*tt8*. T_1s were grown for 14 days on ½ MS agar plates containing 50µg/mL hygromycin for
605 selection. T_1s were genotyped using primers to amplify the region spanning both gRNA targets
606 and by sequencing the PCR products. Lines containing desirable mutations were propagated until
607 homozygous for the mutation and the absence of transgenic elements. Tiling PCR was used to
608 confirm the complete absence of CRISPR-CAS9 in the final lines.

609

610 **Image analysis**

611 Whole seedlings were laid out on an MS agar plate with a ruler in the same plane as the
612 plants. The plate was backlit with a lightboard and imaged with an overhead-mounted camera.
613 Hypocotyls were individually measured using ImageJ.

614 Rosettes were photographed with an overhead-mounted camera on the indicated day. A
615 color card was included in every image to serve as a size reference and allow for color correction
616 if necessary. Images were processed with PlantCV (v 4.2.1) by white balancing each image and
617 then thresholding to isolate the plant from the background (Gehan et al. 2017). The analyze.size
618 function was used to measure shape characteristics and size. The chip size of the color card was
619 measured using the transform.detect_color_card function. The chip size in pixels was used to
620 convert appropriate results to metric measurements.

621 Mini-fields were imaged with an overhead-mounted camera with a color card in every
622 image. Machine learning was used to train the naive.bayes function of PlantCV to distinguish
623 between the plant and background. Only plant and background material within the perimeter of
624 the mini-field box was used to calculate percent ground cover.

625

626 **Density trials**

627 Holes were drilled into Sterilite 27 L boot boxes measuring 59.7 cm L x 42.9 cm W x
628 14.9 cm H for drainage, and each is considered a mini-field. Three independent mini-fields of
629 each planting density and genotype were arranged at random in the greenhouse. Seeds were
630 broadcast, allowing for random spacing of seeds. The mini-fields were grown for 2 weeks to
631 allow seeds to germinate before vernalizing for 3 weeks. The mini-fields were fertilized once a
632 week in the greenhouse.
633 Fields were imaged every 5 days after vernalization. Inflorescences were counted using
634 the cell-counter ImageJ plugin to score open and unopened inflorescences. After senescence, the
635 entire mini-field was harvested to calculate total yield per mini-field.
636
637 **Chlorophyll Fluorescence measurements**
638 Seeds were sown and grown in long day conditions for 7 days, then changed to the
639 appropriate treatment condition and grown for an additional 14 days. Rosettes were imaged with
640 the PhenoVation CropReporter imaging system. Plants were dark-adapted for a minimum of 20
641 minutes before imaging. NPQ, NDVI, and color analysis were taken. Each indice was quantified
642 using the corresponding function in PlantCV.
643
644 **Freezing trial**
645 MN106 and *pif7-1* were grown under controlled conditions in a growth chamber
646 maintained at 22°C with a 16-hour light/8-hour dark photoperiod. Seedlings were grown for two
647 weeks at 22°C before being transferred to a vernalization chamber set at 4°C with an 8-hour
648 light/16-hour dark photoperiod for three weeks to induce cold acclimation. The experiment was
649 repeated across five independent batches, each consisting of 12 seedlings per genotype, resulting
650 in a total of 60 seedlings per line for survival evaluation.
651 Following cold acclimation, seedlings were transferred to a programmable environmental
652 chamber (LU-113, Espec Corp., Hudsonville, MI, USA) for the freezing treatment. Plants were
653 initially held at 4°C for 30 minutes, followed by a gradual temperature reduction at a rate of 2°C
654 per hour until reaching -3°C. This temperature was maintained for 16 hours to promote ice
655 nucleation and pre-freezing conditioning. Subsequently, the temperature was further decreased to
656 -10°C at the same rate (2°C per hour), and plants were held at this target freezing temperature for
657 2 hours. After freezing, the temperature was gradually increased back to 4°C at 2°C per hour,

658 where plants were held for 1 hour before being returned to standard growth conditions (22°C, 16-
659 hour light/8-hour dark) for recovery.
660 Plant survival was assessed 1–2 weeks post-treatment, based on visible regrowth and
661 meristem viability. Plants were considered "survived" if new leaf growth emerged and the
662 meristem remained viable. This experimental design enabled a comparative assessment of freezing
663 tolerance between MN106 wild-type and *pif7* mutant lines under controlled freezing conditions.
664
665 **Seed oil content**
666 Total seed oil content and moisture were determined by nondestructive TD-NMR on 450
667 mg samples of whole pennycress seed using a Bruker MQ40 and Minispec Plus version 7.0.0
668 software to calculate weight percent oil and moisture. TD-NMR was performed on the samples
669 and standards with a Bruker Minispec MQ40 with a 39.95 MHz NMR frequency and 40°C
670 magnet temperature. The 90° and 180° pulse lengths were 11.48 µs and 22.98 µs, respectively.
671 A 23° detection angle, gain of 44 dB, pulse attenuation of 15 dB, recycle delay of 2 s, window 1
672 of 0.055 ms, window 2 (τε) of 7 ms, and 724 magnetic field steps were set to employ a Hahn
673 spin echo effect for signal collection. Each sample employed 16 scans at a receiver gain of 59.
674 Weight percent oil and moisture calibration curves were constructed within the Bruker software
675 for oil standards (20% - 40% oil) and moisture levels (6% - 11% moisture). For sample analysis,
676 450 mg of whole pennycress seed was placed into 10 mm flat-bottom NMR tubes, tempered at
677 40°C in a heat block for 30 minutes, and scanned in the MQ40. The Minispec Plus software
678 applied the standard curves, and the results were exported to Excel. The percent oil on a dry
679 weight basis was calculated by dividing the milligrams of oil in each sample by the dry weight of
680 each sample and multiplying by 100.
681
682 **Funding**
683 This study was supported by the U.S. Department of Energy, Office of Science, Office of
684 Biological and Environmental Research, Genomic Science Program grant no. DE-SC0021286 to
685 DAN, WP, NH and KS.
686
687
688 **Author contributions**

Vanessica Jawahir and Dmitri Nusinow designed this project. Vanessica Jawahir wrote the manuscript, designed, performed, and analyzed experiments. Salma Adam performed and analyzed experiments. Marcus Griffiths collected and analyzed soil cores, and drone images and root morphology in field and controlled experiments. Tad Wesley and Win Phippen designed and performed the in-field density experiment and collected drone images throughout the field season. Wesley and Phippen assisted with all field sample collections and analyzed seed oil content. Nicholas Heller provided the field conditions to measure light. Bhabesh Borphukan and Karen Sanguinet designed and performed the freezing tolerance experiment. All authors edited and reviewed the manuscript.

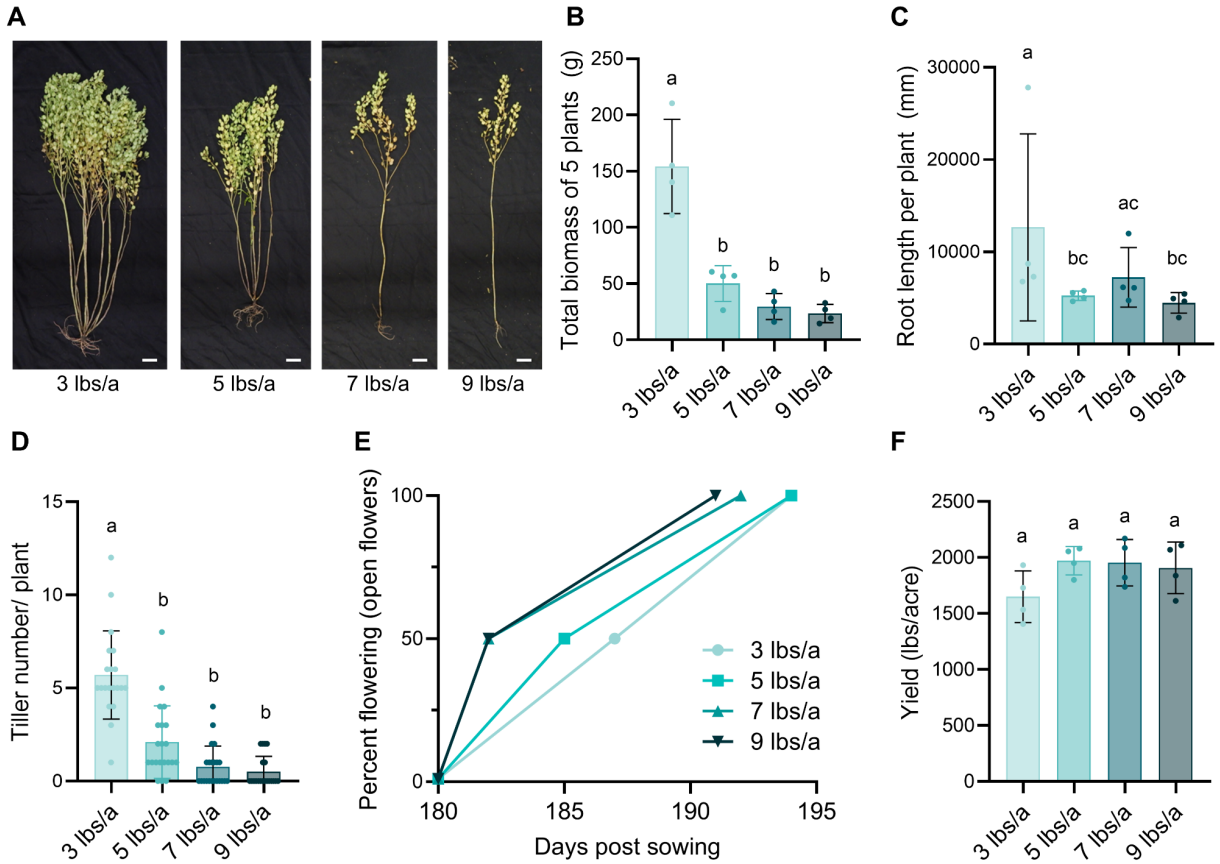

Figure 1. Biomass and yield negatively correlate with seeding density. **(A)** Four plots were sown at 3, 5, 7, and 9 lbs/a. At maturity, plants were harvested from the middle of the plot and imaged. Representative images of individuals from plots are shown. **(B)** Total dried biomass of 5 plants taken from each plot. Statistical significance determined by 2-tailed Welch's t-test (n=4, $p<0.05$). **(C)** Total root length per plant was determined from soil cores from the middle of each plot. Rhizovision Explorer measured root length per core and divided by the number of tap roots present. Statistical significance determined by 2-tailed Mann-Whitney test (n=4, $p<0.05$) **(D)** The number of tillers per plant was counted from harvested individuals. Statistical significance determined by 2-tailed Mann-Whitney test. ($n \geq 20$, $p<0.05$). **(E)** Plots were scored for the dates when each reached 50% and 100% flowering. **(F)** Plots were harvested, and the yield for each plot was determined. Statistical significance determined by 2-tailed Welch's t-test (n=4, $p<0.05$). Common letters indicated no significant difference.

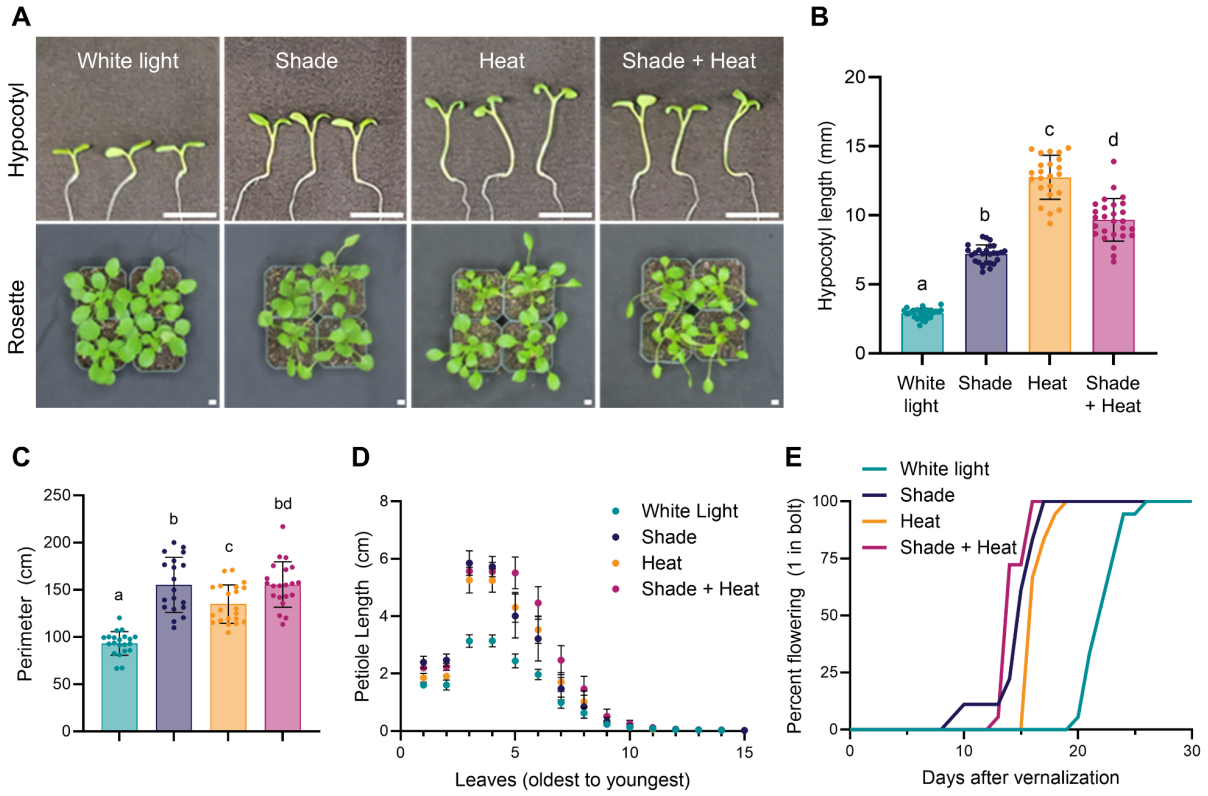

Figure 2. Pennycress increases responses to shade and elevated temperatures. **(A)** Elongation of 5-d-old seedlings grown in white light, shade, heat, and shade + heat. Rosette morphology of plants treated for 6 d with shade, heat, or shade + heat. Scale bar = 1 cm. **(B)** Hypocotyl length of 5-d-old seedlings grown in the indicated treatment for 3 d. Statistical significance determined by 2-tailed Welch's t-test (± SD, n ≥ 23, $p < 0.05$). **(C)** Perimeter of 3-week-old rosettes grown in white light, shade, heat, or shade + heat for 14 d. Statistical significance determined by 2-tailed Welch's t-test (± SD, n ≥ 19, $p < 0.05$). **(D)** Petiole length of each leaf of a 17-d-old rosette treated for 7 d. Leaves 1 and 2 are cotyledons (n = 14). **(E)** Number of days till flowering. Plants were considered flowering when the bolt ≥ 1 inch (n= 18).

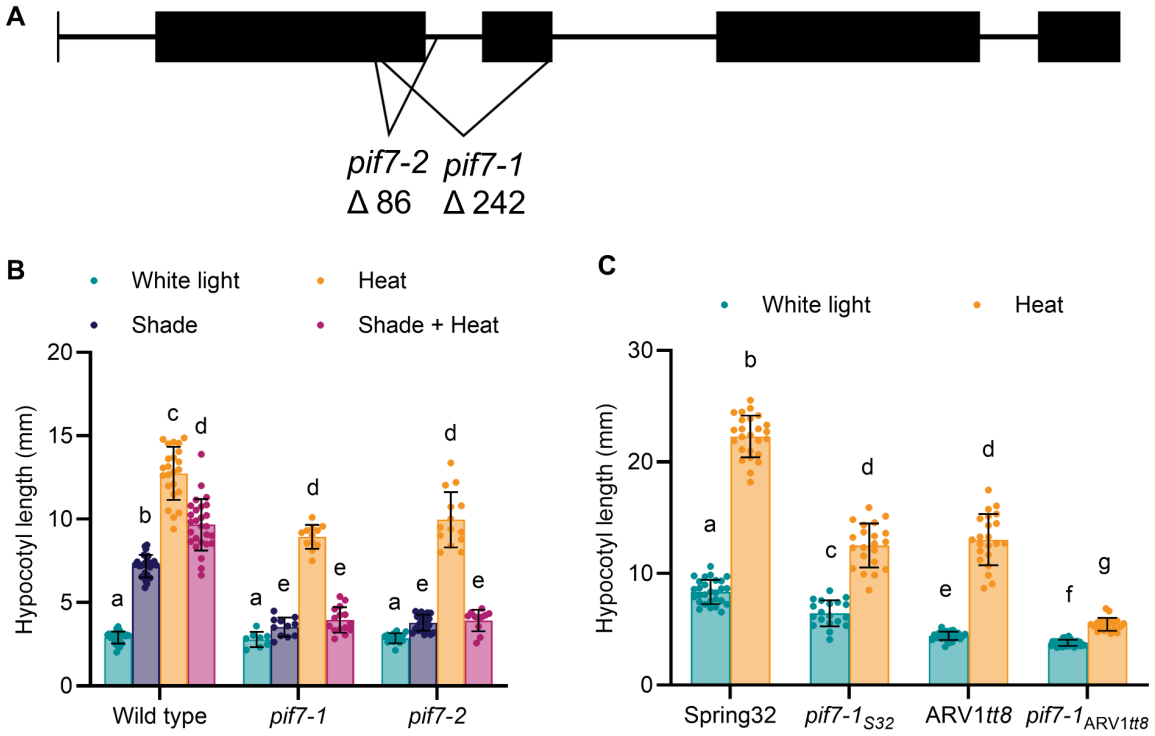

Figure 3. *pif7* has reduced hypocotyl elongation across genetic backgrounds in response to shade and heat. **(A)** PIF7 gene diagram depicting mutations. Exons are black boxes. *pif7-1* and *pif7-2* were generated with CRISPR in the MN106 wild-type background. **(B)** Hypocotyl length of 5-day-old seedlings. Seeds were germinated in white light for 2 d, then grown in shade, heat, or shade + heat, for an additional 3 d. Statistical significance determined by 2-tailed Welch's t-test (± SD, n ≥ 8, $p < 0.05$). Data for wild type is replotted from Figure 2B for comparison. **(C)** Hypocotyl length of 5 d-old seedlings, germinated in white light for 2 d, then grown in heat for an additional 3 d. Statistical significance determined by 2-tailed Welch's t-test (± SD, n ≥ 19, $p < 0.05$). Common letters indicated no significant difference.

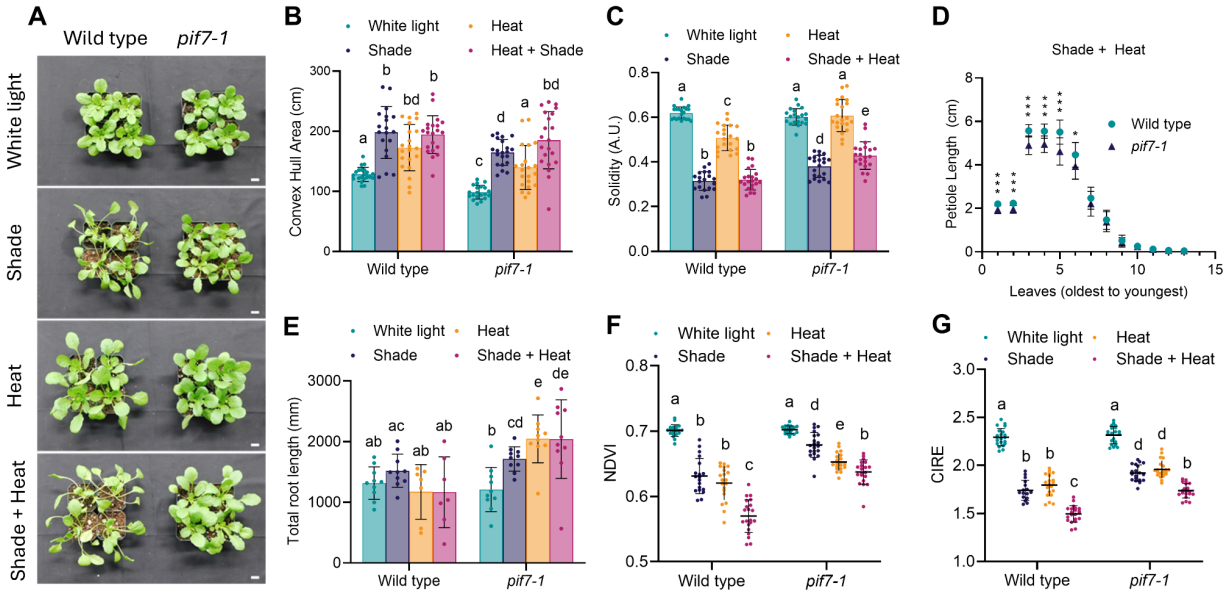

Figure 4. *pif7* attenuates responses to foliar shade and heat throughout vegetative growth. **(A)** Representative plants grown in control conditions for 7 d, then for 14 d in treatment conditions and imaged. **(B)** Rosette solidity of plants grown in control conditions for 7 d, then for 14 d in treatment conditions. Solidity was determined using the shape analysis function from PlantCV. **(C)** The convex hull area of rosettes was calculated using the shape analysis function from PlantCV. **(D)** Petiole length of each leaf of plants grown in control conditions for 10 d, then moved to shade + heat environment for an additional 8 d. Plants were dissected to measure the petiole length of each leaf. Leaves are arranged oldest to youngest; cotyledons are leaves 1 and 2. Statistical significance was determined by 2-tailed Welch's t-test (± SD, n = 14, p* < 0.05, p** < 0.01, p*** <0.001). **(E)** Total root length of plants grown on MS plates for 7 d, then transferred to turface. Plants were then grown in treatment conditions for 10 d. Roots were washed, scanned, and analyzed with Rhizovision (± SD, n ≥ 7, p < 0.05). **(F)** Seeds were sown in soil and grown in long day control conditions (22 °C, 200 µmol m^{-2} s^{-1}, R:Fr =12) for 7 d. On day 7, conditions were changed to shade (22 °C, 200 µmol m^{-2} s^{-1}, R:Fr = 0.3), heat (28 °C, 200 µmol m^{-2} s^{-1}, R:Fr =12) or shade + heat (28 °C, 200 µmol m^{-2} s^{-1}, R:Fr = 0.3). Elevated temperature and the far-red ratio were maintained only during the day. Normalized Difference Vegetation Index (NDVI) and **(G)** chlorophyll index-red edge (CIRE) were measured in dark-adapted plants after 14 d of being grown in the indicated environment. Statistical significance was determined by a 2-tailed Welch's t-test (±SD, n ≥16, p < 0.05). Common letters indicated no significant difference.

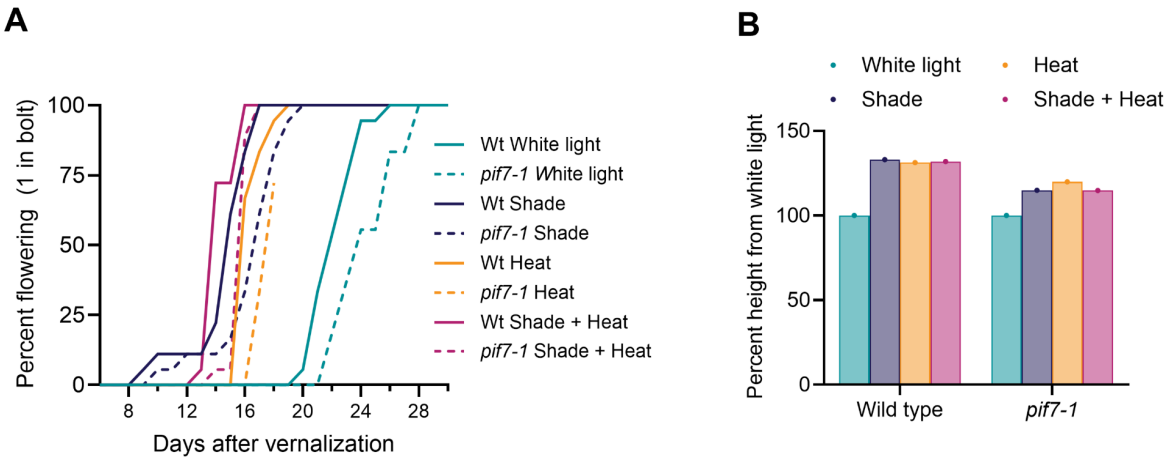

Figure 5. *pif7* attenuates responses to foliar shade and heat through reproductive phases. **(A)** Flowering time of plants grown for 1 week, vernalized for 3 weeks, then moved back to control conditions for 5 d. Plants were then transferred to the indicated treatment condition for 14 d before returning to control conditions. Plants were scored as flowering when bolt height reached one inch (n = 18). **(B)** Plant height was measured at maturity. Height was normalized to plants grown under white light for the duration of the experiment (n ≥ 16).

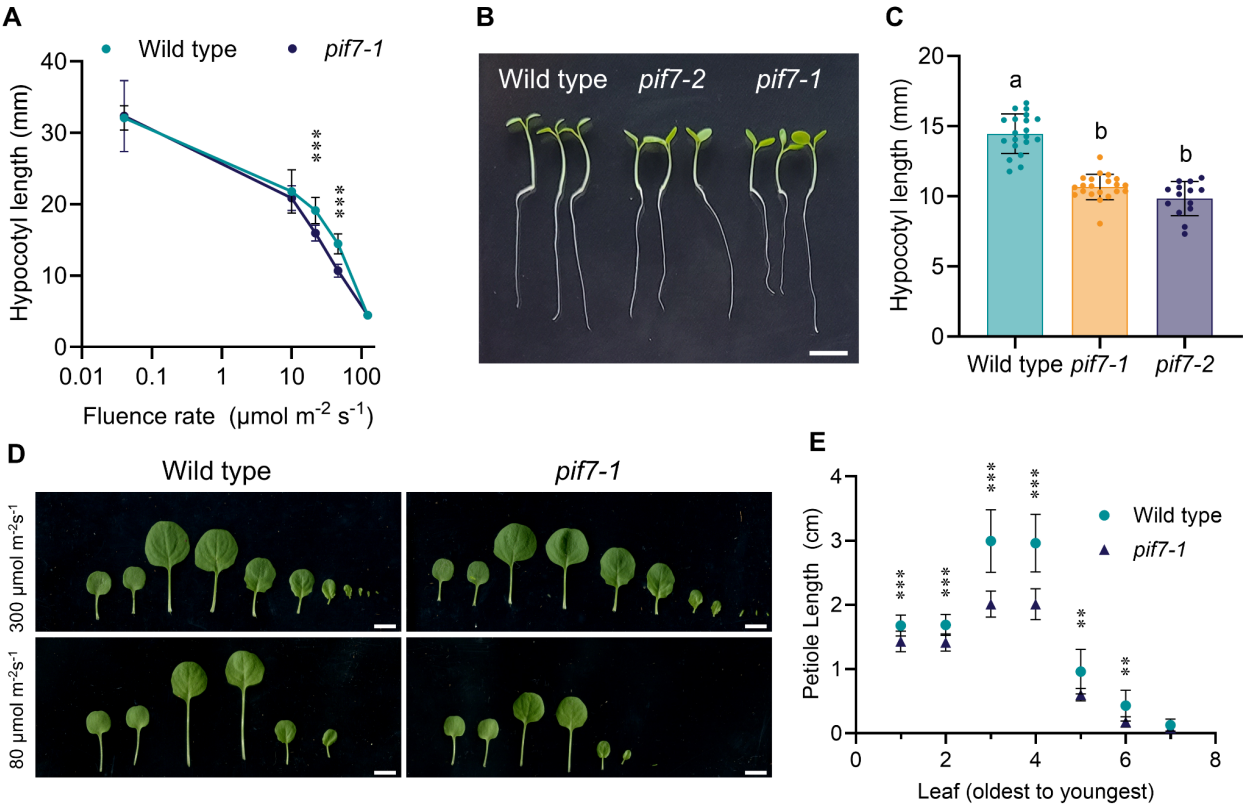

Figure 6. *pif7* has reduced organ elongation in low fluence conditions **(A)** Seedlings were germinated in white light at 120 μmol m^{-2} s^{-1} for 2 d. On day 3, seedlings were grown under various neutral density filters to reduce PAR. Hypocotyls were measured on day 6. Statistical significance was determined by 2-tailed Welch's t-test. (± SD, n ≥ 14, p* < 0.05, p** < 0.01, p*** <0.001) **(B)** Representative hypocotyls at 45 μmol m^{-2} s^{-1}. Scale bar = 5 mm. **(C)** Hypocotyl length of seedlings germinated at 120 μmol m^{-2} s^{-1} for 2 d then grown under 45 μmol m^{-2} s^{-1} for an additional 4 d. Statistical significance was determined by 2-tailed Welch's t-test (± SD, n ≥ 14, p < 0.05). **(D)** Representative leaves of plants grown under control light and low light conditions. Plants were sown and grown for 1 week at 300 μmol m^{-2} s^{-1}. Half of the plants were moved to 80 μmol m^{-2} s^{-1} of light and grown for an additional week, the other half was kept under control light conditions. On day 15, all plants were dissected. Leaves were arranged from oldest to youngest. Scale bar = 1 cm **(E)** Petiole length of each leaf of wild type and *pif7-1* grown at 80 μmol m^{-2} s^{-1}. Statistical significance determined by 2-tailed Welch's t-test (± SD, n ≥ 14, p* < 0.05, p** < 0.01, p*** <0.001). Common letters indicated no significant difference.

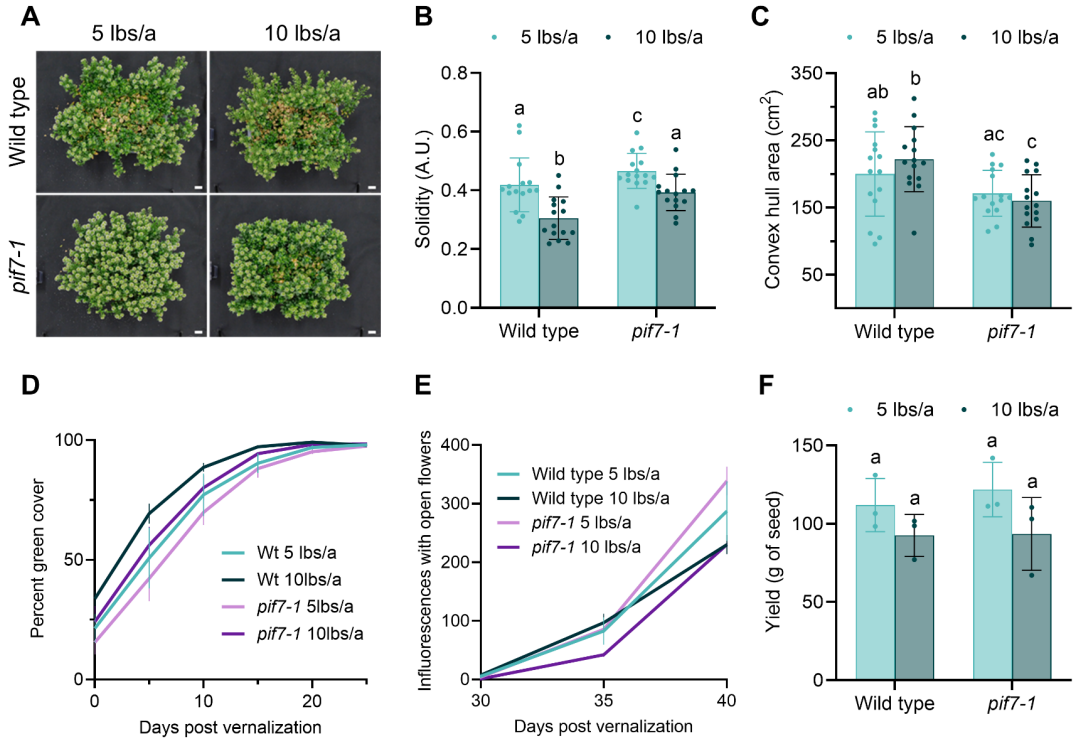

Figure 7. *pif7* attenuates elongation when grown at high density without reducing yield. MN106 and *pif7-1* seeds were sown in 27 L Sterilite containers measuring 59.7 cm x 42.9 cm x 14.9 cm at 5 and 10 lbs/a. The mini fields were grown for 2 weeks, vernalized for 21 d, moved back to standard growing conditions, and imaged every 5 d. **(A)** Mini-fields 40 d after vernalization. **(B)** Five rosettes were pulled randomly from each mini field 11 d after vernalization. Solidity and **(C)** Convex hull area was calculated using the morphology function from PlantCV. Statistical significance determined by 2-tailed Mann-Whitney test (±SD, n = 15, $p < 0.05$). **(D)** Percent green coverage within the boundary of the mini-field was calculated from overheard images taken every 5 days post-vernalization with PlantCV. **(E)** Inflorescences with open flowers were counted in each mini-field. **(F)** All seeds were harvested for each mini-field to calculate average yield. Statistical significance determined by 2-tailed Mann-Whitney test (±SD, n = 3, $p < 0.05$). Common letters indicated no significant difference.

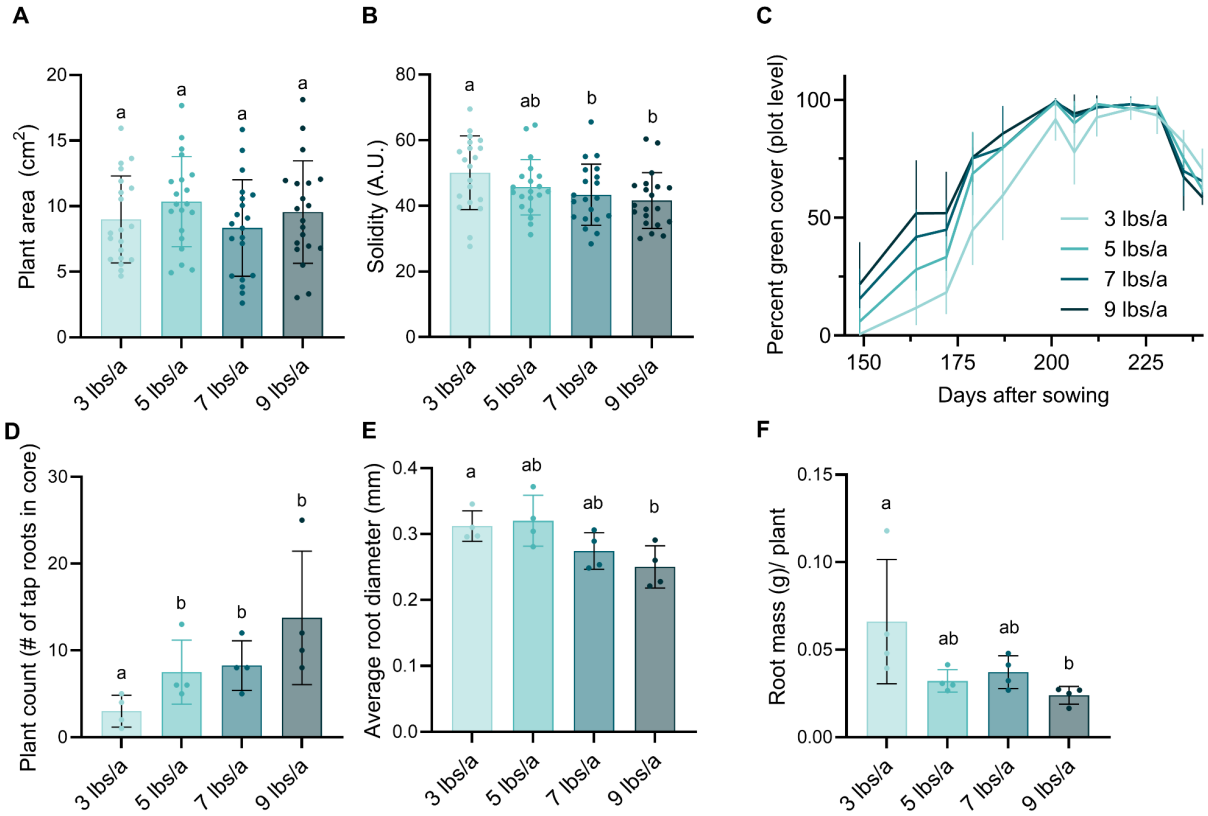

Supplemental Figure 1. Additional field measurements. Five individuals were removed from each density plot and imaged on 12-04-2023, 64 days after planting. **(A)** Plant area and **(B)** solidity were calculated using the shape analysis function from PlantCV. Statistical significance was determined using a 2-tailed Mann-Whitney test (±SD, n = 16, $p < 0.05$). **(C)** The percent green cover of each plot was calculated using drone images to estimate plant coverage of the soil. **(D)** Soil cores were taken from the center of each plot. Tap roots from each core were counted to measure the number of plants per core. Statistical significance was determined using a 2-tailed Wilcoxon rank sum test (±SD, n = 4, $p < 0.05$). **(E)** Root traits were measured using Rhizovision. The root diameter of all roots in the core was averaged. Statistical significance was determined using a 2-tailed Wilcoxon rank sum test (±SD, n = 4, $p < 0.05$). **(F)** Roots were washed and tried to measure biomass. Total biomass was divided by the number of tap roots in the core to estimate root mass per plant. Statistical significance was determined using a 2-tailed Wilcoxon rank sum test (±SD, n = 4, $p < 0.05$).

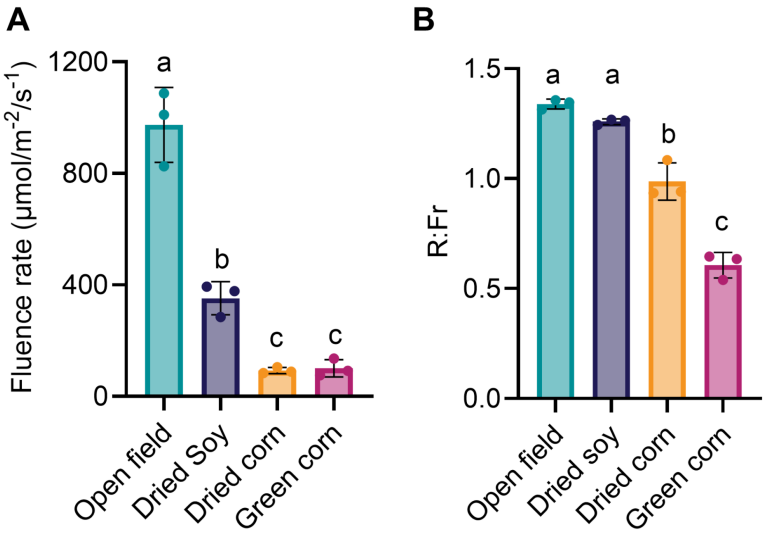

Supplemental Figure 2. Light intensity and quality are altered in interseeded fields and affect yield. **(A)** Light intensity and **(B)** quality were measured on a partly cloudy day on 10-23-2023 between 1- 3 pm with an Li-180. Standing corn measured approximately 9 ft in height. Light readings were taken by walking down a straight line and taking 10-12 measurements approximately every 10 feet. These measurements were averaged for each repetition, n=3. Statistical significance was determined using 2-tailed Welch's t-test (±SD, n = 3, $p < 0.05$). Common letters indicated no significant difference

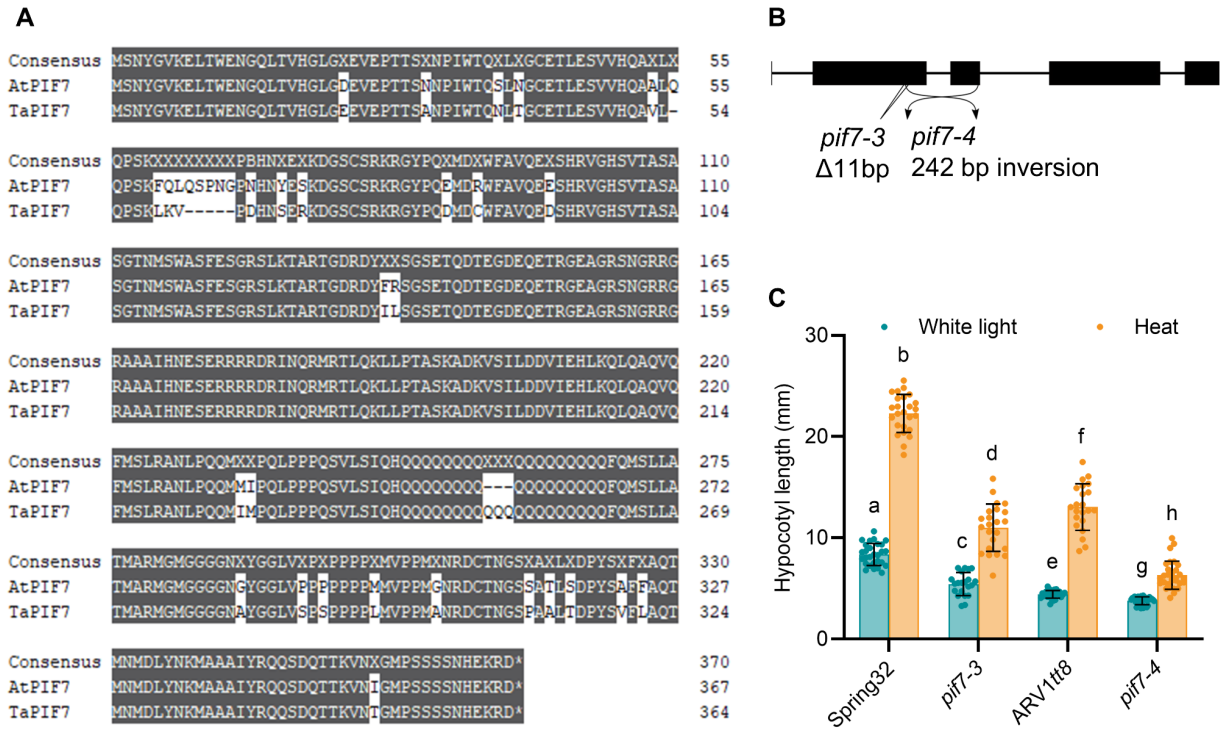

Supplemental Figure 3. (A) *Thlaspi arvense* PIF7 (TaPIF7) is highly similar to *Arabidopsis thaliana* PIF7 (AtPIF7), and *pif7* has reduced elongation in heat. **(A)** Amino acid alignment of pennycress PIF7 (TaPIF7) and Arabidopsis PIF7 (AtPIF7). Agreements with the consensus are highlighted. **(B)** PIF7 gene diagram depicting additional alleles generated by CRISPR-CAS9. Exons are black boxes. *pif7-3,* in the Spring32 genetic background, is a small deletion of 11 bases that results in a frameshift. *pif7-4*, in the ARV1*tt8* background, is an inversion of the gene sequence between the gRNA targets. **(C)** Hypocotyl length of 5 d-old seedlings, germinated in white light for 2 d, then grown in heat for an additional 3 d. Statistical significance determined by 2-tailed Welch's t-test (± SD, $n \geq 21$, $p < 0.05$). Common letters indicated no significant difference.

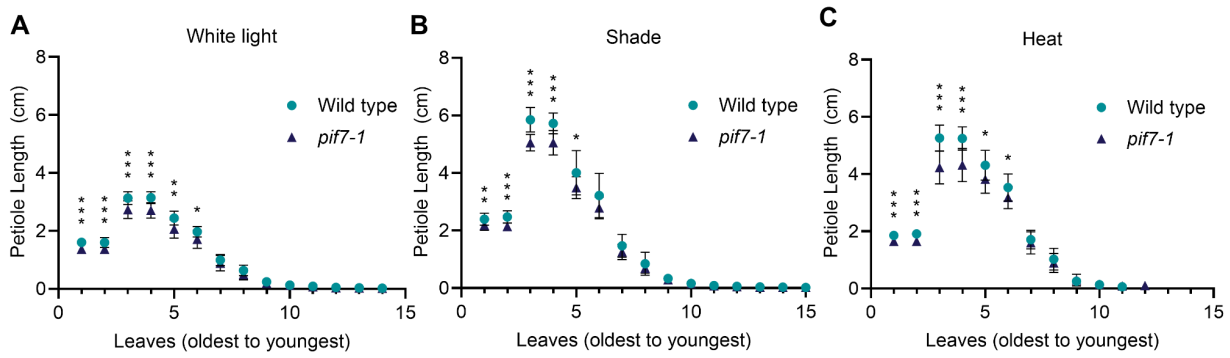

Supplemental Figure 4. *pif7-1* has reduced responses to environmental conditions. Petiole length was measured for each leaf of a rosette grown in **(A)** white light, **(B)** shade, and **(C)** heat. Plants were initially grown in control conditions for 10 d before moving to treatment conditions for 8 d before dissection. Leaves are arranged oldest to youngest; cotyledons are leaves 1 and 2. Statistical significance was determined by 2-tailed Welch's t-test (± SD, n = 14, p* < 0.05, p** < 0.01, p*** <0.001).

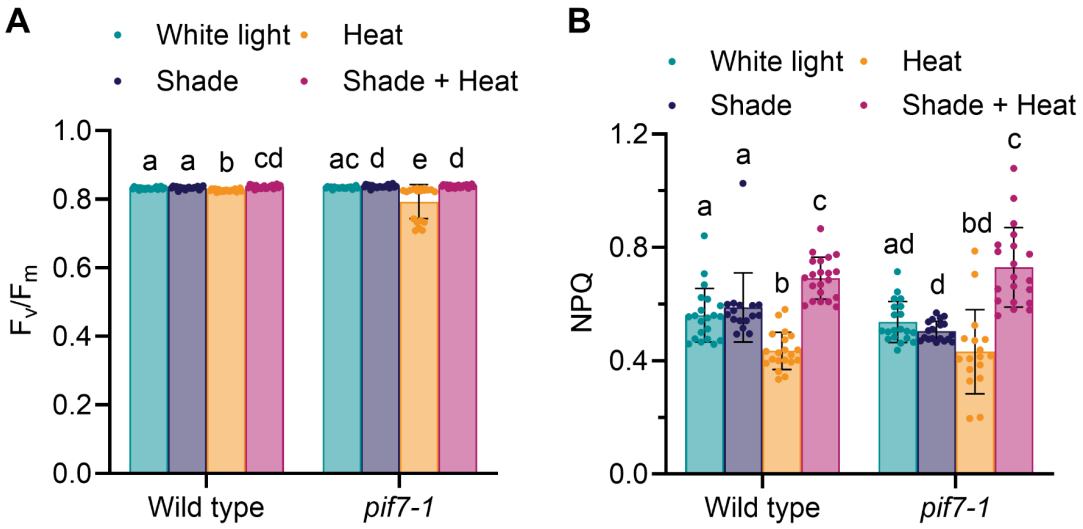

Supplemental Figure 5. Chlorophyll fluorescence measurements of plants grown in shade and heat. **(A)** F_v/F_m and **(B)** NPQ were measured in dark adapted plants after 14 d of being grown in the indicated environment. Seeds were sown in soil and grown in long day control conditions (22 °C, 200 µmol m^{-2} s^{-1}, R:Fr =12) for 7 d. On day 7, conditions were changed to shade (22 °C, 200 µmol m^{-2} s^{-1}, R:Fr = 0.3), heat (28 °C, 200 µmol m^{-2} s^{-1}, R:Fr =12) or shade + heat (28 °C, 200 µmol m^{-2} s^{-1}, R:Fr = 0.3). Elevated temperature and the far-red ratio were maintained only during the day. Statistical significance was determined by a 2-tailed Welch's t-test (±SD, n ≥16, $p < 0.05$). Common letters indicated no significant difference.

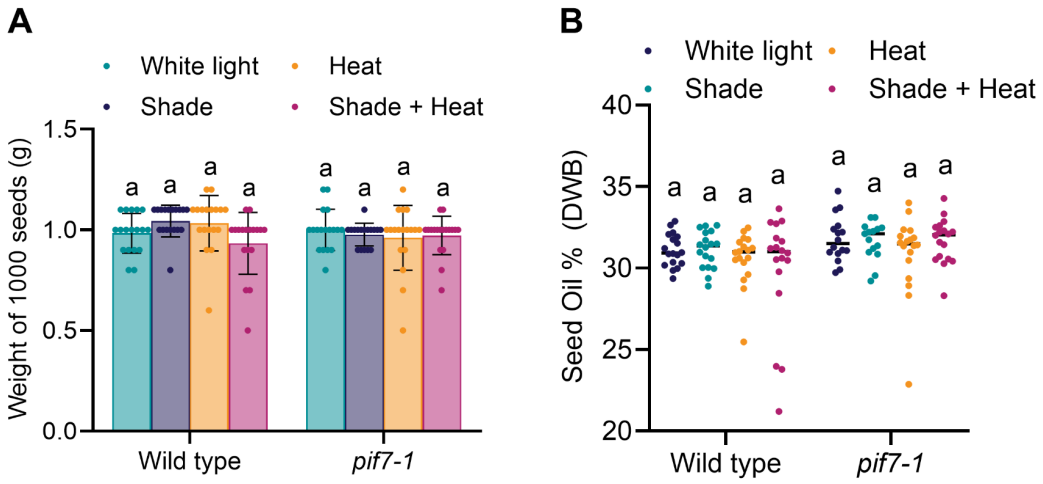

Supplemental Figure 6. *pif7* does not alter seed weight and oil content. Plants at the rosette state were transferred to the indicated condition for 14 d after vernalization, then moved back to control conditions to mature before seeds were harvested and measured. (A) One thousand seeds from each plant were weighed. Statistical significance was determined by 2-tailed Mann-Whitney test (± SD, $n \geq 17$, $p < 0.05$). (B) Seed oil percentage on a dry weight basis (DWB) was measured in seeds. Statistical significance was determined by 2-tailed Mann-Whitney test (± SD, $n \geq 15$, $p < 0.05$).

882

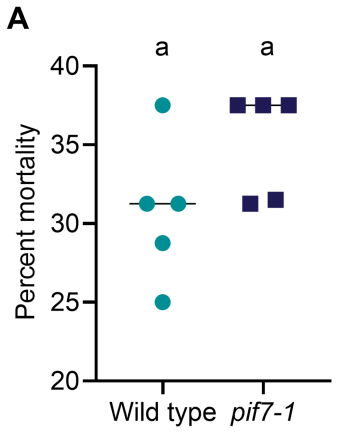

883

884

885 **Supplemental Figure 7.** *pif7* maintains freezing tolerance. Plants were grown for 2
886 weeks, vernalized for 3 weeks at 4 °C, then subjected to freezing treatment down to -10
887 °C. Plants were returned to the greenhouse and evaluated for survival after a 10 d
888 recovery period. 16 plants of each genotype were tested for freezing tolerance in 5
889 independent tests. Statistical significance was determined by a 2-tailed Mann-Whitney
890 test (± SD, $n \geq 5$, $p < 0.05$). Common letters indicated no significant difference.

References

Arief, M.A.A. et al., 2023. Chlorophyll fluorescence imaging for early detection of drought and heat stress in strawberry plants. *Plants*, 12(6), p.1387.

Assefa, Y. et al., 2018. Analysis of long term study indicates both agronomic optimal plant density and increase maize yield per plant contributed to yield gain. *Scientific reports*, 8(1), p.4937.

Balcerowicz, M., 2020. PHYTOCHROME-INTERACTING FACTORS at the interface of light and temperature signalling. *Physiologia plantarum*, 169(3), pp.347–356.

Bauer, D. et al., 2004. Constitutive photomorphogenesis 1 and multiple photoreceptors control degradation of phytochrome interacting factor 3, a transcription factor required for light signaling in Arabidopsis. *The Plant cell*, 16(6), pp.1433–1445.

Bishop, L. & Nelson, K.A., 2019. Field pennycress seeding date and corn herbicide management effects on corn, pennycress, and soybean production. *Agronomy journal*, 111(1), pp.257–263.

Burko, Y. et al., 2022. PIF7 is a master regulator of thermomorphogenesis in shade. *Nature communications*, 13(1), p.4942.

Cao, Y. et al., 2022. Leaf angle: a target of genetic improvement in cereal crops tailored for high-density planting. *Plant biotechnology journal*, 20(3), pp.426–436.

Casal, J.J. & Balasubramanian, S., 2019. Thermomorphogenesis. *Annual review of plant biology*, 70(1), pp.321–346.

Casal, J.J. & Fankhauser, C., 2023. Shade avoidance in the context of climate change. *Plant physiology*, 191(3), pp.1475–1491.

Cerdán, P.D. & Chory, J., 2003. Regulation of flowering time by light quality. *Nature*, 423(6942), pp.881–885.

Clack, T., Mathews, S. & Sharrock, R.A., 1994. The phytochrome apoprotein family in Arabidopsis is encoded by five genes: the sequences and expression of PHYD and PHYE. *Plant molecular biology*, 25(3), pp.413–427.

Cubins, J.A. et al., 2019. Management of pennycress as a winter annual cash cover crop. A review. *Agronomy for sustainable development*, 39(5), pp.1–11.

Delker, C., Quint, M. & Wigge, P.A., 2022. Recent advances in understanding thermomorphogenesis signaling. *Current opinion in plant biology*, 68(102231), p.102231.

Dorn, K.M. et al., 2015. A draft genome of field pennycress (Thlaspi arvense) provides tools for the domestication of a new winter biofuel crop. *DNA research: an international journal for*

rapid publication of reports on genes and genomes, 22(2), pp.121–131.

Dose, H.L. et al., 2017. Early planting dates maximize winter annual field pennycress (Thlaspi arvense L.) yield and oil content. *Industrial crops and products*, 97, pp.477–483.

Duvick, D.N., 2005. The Contribution of Breeding to Yield Advances in maize (Zea mays L.). In *Advances in Agronomy*. Advances in agronomy. Elsevier, pp. 83–145.

Elli, E.F. et al., 2023. Maize leaf angle genetic gain is slowing down in the last decades. *Crop science*, 63(6), pp.3520–3533.

Fan, J. et al., 2013. A life cycle assessment of pennycress (Thlaspi arvense L.) -derived jet fuel and diesel. *Biomass and Bioenergy*, 55, p.87.

Fernández, V. et al., 2016. Photoperiodic and thermosensory pathways interact through CONSTANS to promote flowering at high temperature under short days. *The Plant journal: for cell and molecular biology*, 86(5), pp.426–440.

Fiorucci, A.-S. et al., 2020. PHYTOCHROME INTERACTING FACTOR 7 is important for early responses to elevated temperature in Arabidopsis seedlings. *The New phytologist*, 226(1), pp.50–58.

Franklin, K.A., 2008. Shade avoidance. *The new phytologist*, 179(4), pp.930–944.

Franklin, K.A. & Whitelam, G.C., 2005. Phytochromes and shade-avoidance responses in plants. *Annals of botany*, 96(2), pp.169–175.

Galvão, V.C. et al., 2019. PIF transcription factors link a neighbor threat cue to accelerated reproduction in Arabidopsis. *Nature communications*, 10(1), p.4005.

Gehan, M.A. et al., 2017. PlantCV v2: Image analysis software for high-throughput plant phenotyping. *PeerJ*, 5, p.e4088.

van Gelderen, K. et al., 2018. Far-red light detection in the shoot regulates lateral root development through the HY5 transcription factor. *The plant cell*, 30(1), pp.101–116.

Ghosh, D., Mohapatra, S. & Dogra, V., 2023. Improving photosynthetic efficiency by modulating non-photochemical quenching. *Trends in plant science*, 28(3), pp.264–266.

Gray, S.B. & Brady, S.M., 2016. Plant developmental responses to climate change. *Developmental biology*, 419(1), pp.64–77.

Griffiths, M., 2025. Images & code for drone image analysis for manuscript on pennycress diversity. Available at: http://dx.doi.org/10.5281/zenodo.15066164 [Accessed April 16, 2025].

Griffiths, M. et al., 2022. Optimisation of root traits to provide enhanced ecosystem services in agricultural systems: A focus on cover crops. *Plant, cell & environment*, 45(3), pp.751–770.

957 Jung, J.-H. et al., 2016. Phytochromes function as thermosensors in Arabidopsis. *Science*,
958 354(6314), pp.886–889.

959 Kami, C. et al., 2010. Light-regulated plant growth and development. *Current topics in*
960 *developmental biology*, 91, pp.29–66.

961 Kidokoro, S. et al., 2009. The phytochrome-interacting factor PIF7 negatively regulates DREB1
962 expression under circadian control in Arabidopsis. *Plant physiology*, 151(4), pp.2046–2057.

963 Kim, R.J.A. et al., 2024. Photobody formation spatially segregates two opposing phytochrome B
964 signaling actions to titrate plant environmental responses. *bioRxiv : the preprint server for*
965 *biology*. Available at: http://dx.doi.org/10.1101/2023.11.12.566724.

966 Koirala, N. et al., 2023. Seed treatment affected establishment and yield in two pennycress lines.
967 *Frontiers in Agronomy*, 5. Available at:
968 https://www.frontiersin.org/journals/agronomy/articles/10.3389/fagro.2023.1205259.

969 Lee, C.-M. & Thomashow, M.F., 2012. Photoperiodic regulation of the C-repeat binding factor
970 (CBF) cold acclimation pathway and freezing tolerance in Arabidopsis thaliana.
971 *Proceedings of the National Academy of Sciences of the United States of America*, 109(37),
972 pp.15054–15059.

973 Legris, M. et al., 2016. Phytochrome B integrates light and temperature signals in *Arabidopsis*.
974 *Science*, 354(6314), pp.897–900.

975 Legris, M., Ince, Y.Ç. & Fankhauser, C., 2019. Molecular mechanisms underlying phytochrome-
976 controlled morphogenesis in plants. *Nature communications*, 10(1), pp.1–15.

977 Li, L. et al., 2012. Linking photoreceptor excitation to changes in plant architecture. *Genes &*
978 *development*, 26(8), pp.785–790.

979 Li, S. et al., 2021. Estimating the contribution of plant traits to light partitioning in simultaneous
980 maize/soybean intercropping. *Journal of experimental botany*, 72(10), pp.3630–3646.

981 Liu, Y., Jafari, F. & Wang, H., 2021. Integration of light and hormone signaling pathways in the
982 regulation of plant shade avoidance syndrome. *aBIOTECH*, 2(2), pp.131–145.

983 Lorrain, S. et al., 2008. Phytochrome-mediated inhibition of shade avoidance involves
984 degradation of growth-promoting bHLH transcription factors. *The Plant journal: for cell*
985 *and molecular biology*, 53(2), pp.312–323.

986 Lu, J. et al., 2023. Row ratio increasing improved light distribution, photosynthetic
987 characteristics, and yield of peanut in the maize and peanut strip intercropping system.
988 *Frontiers in plant science*, 14, p.1135580.

989 Maxwell, K. & Johnson, G.N., 2000. Chlorophyll fluorescence—a practical guide. *Journal of*
990 *experimental botany*, 51(345), pp.659–668.

991 McGinn, M. et al., 2019. Molecular tools enabling pennycress (Thlaspi arvense) as a model plant
992 and oilseed cash cover crop. *Plant biotechnology journal*, 17(4), pp.776–788.

993 Mohammed, Y.A. et al., 2020. Establishing winter annual cover crops by interseeding into Maize
994 and Soybean. *Agronomy journal*, 112(2), pp.719–732.

995 Moser, B.R., 2012. Biodiesel from alternative oilseed feedstocks: camelina and field pennycress.
996 *Biofuels*, 3(2), pp.193–209.

997 Moser, B.R., Evangelista, R.L. & Isbell, T.A., 2016. Preparation and Fuel Properties of Field
998 Pennycress (Thlaspi arvense) Seed Oil Ethyl Esters and Blends with Ultralow-Sulfur Diesel
999 Fuel. *Energy & fuels: an American Chemical Society journal*, 30(1), pp.473–479.

1000 Murchie, E.H. & Lawson, T., 2013. Chlorophyll fluorescence analysis: a guide to good practice
1001 and understanding some new applications. *Journal of experimental botany*, 64(13),
1002 pp.3983–3998.

1003 Nozue, K. et al., 2007. Rhythmic growth explained by coincidence between internal and external
1004 cues. *Nature*, 448(7151), pp.358–361.

1005 Nunn, A. et al., 2022. Chromosome-level Thlaspi arvense genome provides new tools for
1006 translational research and for a newly domesticated cash cover crop of the cooler climates.
1007 *Plant biotechnology journal*, 20(5), pp.944–963.

1008 Oravec, M.W. & Greenham, K., 2022. The adaptive nature of the plant circadian clock in natural
1009 environments. *Plant physiology*, 190(2), pp.968–980.

1010 Pantazopoulou, C.K., Bongers, F.J. & Pierik, R., 2021. Reducing shade avoidance can improve
1011 Arabidopsis canopy performance against competitors. *Plant, cell & environment*, 44(4),
1012 pp.1130–1141.

1013 Park, E. et al., 2012. Phytochrome B inhibits binding of phytochrome-interacting factors to their
1014 target promoters. *The Plant journal: for cell and molecular biology*, 72(4), pp.537–546.

1015 Park, E., Kim, Y. & Choi, G., 2018. Phytochrome B Requires PIF Degradation and Sequestration
1016 to Induce Light Responses across a Wide Range of Light Conditions. *The Plant cell*, 30(6),
1017 pp.1277–1292.

1018 Park, J., Bae, S. & Kim, J.-S., 2015. Cas-Designer: a web-based tool for choice of CRISPR-Cas9
1019 target sites. *Bioinformatics* , 31(24), pp.4014–4016.

1020 Patel, S. et al., 2021. Interseeded pennycress and camelina yield and influence on row crops.
1021 *Agronomy journal*, 113(3), pp.2629–2647.

1022 Paulišić, S. et al., 2021. Adjustment of the PIF7-HFR1 transcriptional module activity controls
1023 plant shade adaptation. *The EMBO journal*, 40(1), p.e104273.

1024 Pham, V.N., Kathare, P.K. & Huq, E., 2018. Phytochromes and Phytochrome Interacting

1025 Factors. *Plant physiology*, 176(2), pp.1025–1038.

1026 Ranganathan, J. et al., 2018. How to Sustainably Feed 10 Billion People by 2050, in 21 Charts.
1027 Available at: https://www.wri.org/insights/how-sustainably-feed-10-billion-people-2050-
1028 21-charts [Accessed November 14, 2024].

1029 Raza, A. et al., 2020. Agro-techniques for lodging stress management in maize-soybean
1030 intercropping system-A review. *Plants*, 9(11), p.1592.

1031 Rockwell, N.C., Su, Y.-S. & Lagarias, J.C., 2006. Phytochrome structure and signaling
1032 mechanisms. *Annual review of plant biology*, 57, pp.837–858.

1033 Roig-Villanova, I. & Martínez-García, J.F., 2016. Plant Responses to Vegetation Proximity: A
1034 Whole Life Avoiding Shade. *Frontiers in plant science*, 7, p.236.

1035 Romero-Montepaone, S. et al., 2020. Shade avoidance responses become more aggressive in
1036 warm environments. *Plant, cell & environment*, 43(7), pp.1625–1636.

1037 Rosado, D. et al., 2022. WRKY transcription factors and ethylene signaling modify root growth
1038 during the shade-avoidance response. *Plant physiology*, 188(2), pp.1294–1311.

1039 Salisbury, F.J. et al., 2007. Phytochrome coordinates Arabidopsis shoot and root development:
1040 Phytochrome coordinates development. *The Plant journal: for cell and molecular biology*,
1041 50(3), pp.429–438.

1042 Schiml, S., Fauser, F. & Puchta, H., 2016. Repair of adjacent single-strand breaks is often
1043 accompanied by the formation of tandem sequence duplications in plant genomes.
1044 *Proceedings of the National Academy of Sciences of the United States of America*, 113(26),
1045 pp.7266–7271.

1046 Schmitt, J., Dudley, S.A. & Pigliucci, M., 1999. Manipulative Approaches to Testing Adaptive
1047 Plasticity: Phytochrome-Mediated Shade-Avoidance Responses in Plants. *The American*
1048 *naturalist*, 154(S1), pp.S43–S54.

1049 Seethepalli, A. et al., 2021. RhizoVision Explorer: open-source software for root image analysis
1050 and measurement standardization. *AoB plants*, 13(6), p.lab056.

1051 Sessa, G. et al., 2018. Multiple pathways in the control of the shade avoidance response. *Plants*,
1052 7(4), p.102.

1053 Sharrock, R.A., 2008. The phytochrome red/far-red photoreceptor superfamily. *Genome biology*,
1054 9(8), p.230.

1055 Sharrock, R.A. & Quail, P.H., 1989. Novel phytochrome sequences in Arabidopsis thaliana:
1056 structure, evolution, and differential expression of a plant regulatory photoreceptor family.
1057 *Genes & development*, 3(11), pp.1745–1757.

1058 Smith, H., 1982. Light quality, photoperception, and plant strategy. *Annual review of plant*

1059 *physiology*, 33(1), pp.481–518.

1060 Stamford, J.D. et al., 2023. Development of an accurate low cost NDVI imaging system for
1061 assessing plant health. *Plant methods*, 19(1), p.9.

1062 Tang, Y.-J. & Liesche, J., 2017. The molecular mechanism of shade avoidance in crops – How
1063 data from Arabidopsis can help to identify targets for increasing yield and biomass
1064 production. *Journal of integrative agriculture*, 16(6), pp.1244–1255.

1065 Us Epa, O., 2021. Climate Change Indicators: Seasonal Temperature. Available at:
1066 https://www.epa.gov/climate-indicators/climate-change-indicators-seasonal-temperature
1067 [Accessed November 21, 2024].

1068 Wille, W. et al., 2017. Reducing shade avoidance responses in a cereal crop. *AoB plants*, 9(5),
1069 p.lx039.

1070 de Wit, M. et al., 2016. Integration of Phytochrome and Cryptochrome Signals Determines Plant
1071 Growth during Competition for Light. *Current biology: CB*, 26(24), pp.3320–3326.

1072 Wollenberg, A.C. et al., 2008. Acceleration of flowering during shade avoidance in Arabidopsis
1073 alters the balance between FLOWERING LOCUS C-mediated repression and photoperiodic
1074 induction of flowering. *Plant physiology*, 148(3), pp.1681–1694.

1075 York, L.M., Nord, E.A. & Lynch, J.P., 2013. Integration of root phenes for soil resource
1076 acquisition. *Frontiers in plant science*, 4, p.355.

1077